Marine Geology 443 (2022) 106673

Contents lists available at ScienceDirect

Marine Geology

journal homepage: www.elsevier.com/locate/margo

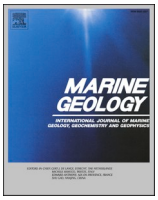

Research Paper

Ichnological evidence for bottom water oxygenation during organic rich layer deposition in the westernmost Mediterranean over the Last Glacial Cycle

Santiago Casanova-Arenillas [a,*], Francisco J. Rodríguez-Tovar [a], Francisca Martínez-Ruiz [b]

[a] Departamento de Estratigrafía y Paleontología, Universidad de Granada, Campus Fuentenueva s/n, 18002, Granada, Spain
[b] Instituto Andaluz de Ciencias de la Tierra, Consejo Superior de Investigaciones Científicas-Universidad de Granada (CSIC-UGR), Avda. de las Palmeras 4, Armilla, 18100 Granada, Spain.

ARTICLE INFO

Editor: Michele Rebesco

Keywords:
Ichnology
Pelagic sediments
Organic matter
Quaternary stratigraphy
Palaeoceanography
Alboran Sea
Mediterranean

ABSTRACT

Organic rich layers (ORLs), deposited in the westernmost Mediterranean over the Last Glacial Cycle, have been studied integrating sedimentological and ichnological information from sediment records recovered at Ocean Drilling Program Leg 161 Sites 976 and 977. The conducted study has served to redefine the ORLs initially differentiated in sediment records from Sites 977 and 976, with seven new ORLs recognized, as well as extensions and subtraction of some parts in the ORLs previously defined. In addition, three different ORL types are distinguished according to sedimentological and ichnological features. Type 1 with intermediate thickness is highly bioturbated, mainly consisting of abundant *Scolicia* and *Planolites*, frequent *Chondrites*, and possible *Thalassinoides* in the base, which are interpreted as supporting dysoxic conditions during deposition. Type 2, corresponding to thicker intervals, shows alternance of highly to moderately bioturbated parts, revealing variable oxygen conditions —from moderate to extreme dysoxic or even suboxic. Type 3 consists of short, laminated intervals characterized by the absence of bioturbation, indicating anoxic or suboxic conditions and determining unfavourable macro benthic habitat. The amended ORLs show a correlation between the Sea Surface Temperatures and established climatic events over the Last Glacial Cycle in the Western Mediterranean.

1. Introduction

The present study is centred on the cyclic deposition of organic carbon rich sediments from the Alboran Sea Basin over the Last Glacial Cycle. We have analysed two sediment records at the East and at the West of Alboran Sea Basin (Fig. 1), which come from two drilling sites from the Leg 161 of the Ocean Drilling Program (ODP).

These organic-rich sediments deposited in the Western Mediterranean are normally called organic-rich layers (ORLs) differentiating them from the Eastern Mediterranean "Sapropels". The studied time interval the Mediterranean spans since the beginning of the penultimate interglacial and Marine Isotope Stage 5, ~130 ka, until the end of the Würn Glaciation over the northern hemisphere, ~11 ka (e.g., Dansgaard et al., 1993). Despite ORLs being layers enriched in Total Organic Carbon (TOC) and cyclically deposited like the sapropels, they are not equivalent layers, probably entailing a more complex set of conditions behind their deposition. ORLs are not always synchronic with sapropels and do not seem to follow the insolation maxima as sapropels do (von Grafenstein et al., 1999; Cacho et al., 2002; Rogerson et al., 2008; Rohling et al., 2015). Whereas sapropels have been extensively studied (among many others, Kidd et al., 1978; Sigl et al., 1978; Rohling and Hilgen, 1991; Rohling, 1994; Cramp and O'Sullivan, 1999; Rohling et al., 2015; Grimm et al., 2015; Grant et al., 2016; Wu et al., 2018), ORLs from the Western Mediterranean are largely unexplored, with the exception of the most recent one, the ORL1 (Bárcena et al., 2001; Cacho et al., 2002; Rogerson et al., 2008; Rodrigo-Gámiz et al., 2011; Jiménez-Espejo et al., 2015; Martínez-Ruiz et al., 2015; Pérez-Asensio et al., 2020). However, ORLs also represent important organic carbon accumulations and record the response of the Mediterranean to palaeoceanographic and climate variability.

In general, most organic matter (OM) in the marine environment is mineralized either from primary productivity or from continental input before its burial; but when production exceeds degradation part of it is preserved in the sediment (e.g., Middelburg et al., 1999; Berner, 2003).

* Corresponding author.
E-mail addresses: scasanova@ugr.es (S. Casanova-Arenillas), fjrtovar@ugr.es (F.J. Rodríguez-Tovar), fmruiz@ugr.es (F. Martínez-Ruiz).

https://doi.org/10.1016/j.margeo.2021.106673
Received 12 May 2021; Received in revised form 5 October 2021; Accepted 14 October 2021
Available online 20 October 2021

The dominant factor in OM preservation has been intensively debated for decades (e.g., Calvert, 1987; Pedersen and Calvert, 1990; Hedges and Keil, 1995; Hedges et al., 1997; Moodley et al., 2005; Arndt et al., 2013; LaRowe et al., 2020) particularly in view of the high variability observed over space and time in the deep ocean (Canfield, 1994; Berner, 2003; Blair and Aller, 2012; Arndt et al., 2013). For instance, past oceans have had generalized O_2 depleted zones in which considerable amounts of OM accumulated and were preserved in the geological records (Jenkyns, 2010). Yet in modern oceans, the presence of large oxygen-depleted areas is limited to a very few places —e.g., the isolated basins of the Black Sea or the Baltic Sea— or the oxygen minimum zones derived from biological productivity that appear in some upwelling continental margins like Namibia or Peru. The amount of OM preserved depends on an interlaced combination of factors, such as the quantity of OM reaching the bottom due to productivity (Emeis et al., 2000), and the velocity of degradation, in turn, related to oxygenation and burial velocity, hence sedimentation rate. Other factors that can affect the degradation of OM include composition, electron acceptor availability, benthic microbial community, physical properties, and macrobenthic activity (e.g., LaRowe et al., 2020). Because the relative importance of these factors varies over time and space, OM rich intervals in the geological record could point to very diverse signatures (e.g., Aller, 1982; Middelburg, 1989, 2018; Mollenhauer et al., 2007; Zonneveld et al., 2010; Arndt et al., 2013; LaRowe et al., 2020). TOC values in the Western Mediterranean can reach values of 2.27%, as registered in the Balear Basin, or 2% in the Alboran Sea Basin, or even values over 6% in the Ionian Sea (Murat, 1999). During ODP Leg 16, the Shipboard scientific party established a limit of 0.8% TOC to define ORLs, contrasting with the values of 2% used during leg 160 of the ODP in the Eastern Mediterranean to define sapropels (Kidd et al., 1978; Murat, 1999, Emeis et al., 2000). Background TOC values found in the Western Mediterranean are also higher than those of the Eastern Basin.

In the Eastern Mediterranean Sea, the simultaneous occurrence of high productivity along with low oxygenation in the bottom waters is held to be the main factor behind sapropel deposition (e.g., Rohling et al., 2015). In the Western Mediterranean, previous work has evidenced that the main factors controlling ORL deposition are productivity and bottom water oxygenation, based on foraminifera, biomarker, and geochemical analysis (Casford et al., 2003; Meyers and Arnaboldi, 2005; Pérez-Asensio et al., 2020, among others). Debate persists about which causes are predominant, or if all events could have the same set of conditions (Rohling et al., 2015). Recent studies in the Western Mediterranean propose that productivity alone cannot produce the low oxygen conditions necessary for ORL deposition, for which reason decreasing deep-water ventilation would also be required (Rogerson et al., 2008; Rodrigo-Gámiz et al., 2011; Pérez-Asensio et al., 2020). The sedimentation rate also influences TOC content and its dilution in the sediment (e.g., Tyson, 2001); however, the fact that it remains high in the Alboran Sea Basin in the studied time would mean it is not a main controlling factor for ORL deposition in this setting.

The deep-water stagnation that leads to ORL deposition has been proposed to be produced by a combination of low aspiration over the Gibraltar Strait (Rogerson et al., 2008; Rohling et al., 2015; Pérez-Asensio et al., 2020) and a decrease in the rate of deep-water sinking over the Gulf of Lion related to buoyancy changes (Millot, 1999; Cacho et al., 2002; Frigola et al., 2008; Rogerson et al., 2008; Pérez-Asensio et al., 2020). Changes in the precipitation-evaporation balance can moreover induce salinization of the superficial waters during certain periods —not necessarily the colder periods— inducing buoyancy variations that could enhance deepwater sinking during warmer phases (Cisneros et al., 2019). Variations in deep-water ventilation are also related to climatic swifts over the northern hemisphere, for example, the ones resulting in Dansgaard-Oeschger and Heinrich events (Sierro et al., 2005; Frigola et al., 2008; Rohling et al., 2015). Despite a reported decrease in ventilation during Heinrich events due to the freshening and decreased density of superficial waters (Sierro et al., 2005; Rogerson et al., 2008; Rohling et al., 2015), which may precondition posterior low oxygenation events, its effect alone would hardly suffice to promote ORL deposition. ORL1 does not show a clear correlation with these events (Rogerson et al., 2008). Variations in the Levantine Intermediate Water have also been invoked to explain the absence of influence of Heinrich events in the ORLs, due to compensation of its possible effects (Rogerson et al., 2008). Still, further investigation is required for reconstructing the palaeoceanographic conditions leading to ORL deposition elsewhere than the ORL1 (14.5–8.5 ka), which has been more profusely studied (Pérez-Folgado et al., 2004; Rogerson et al., 2008; Bazzicalupo et al.,

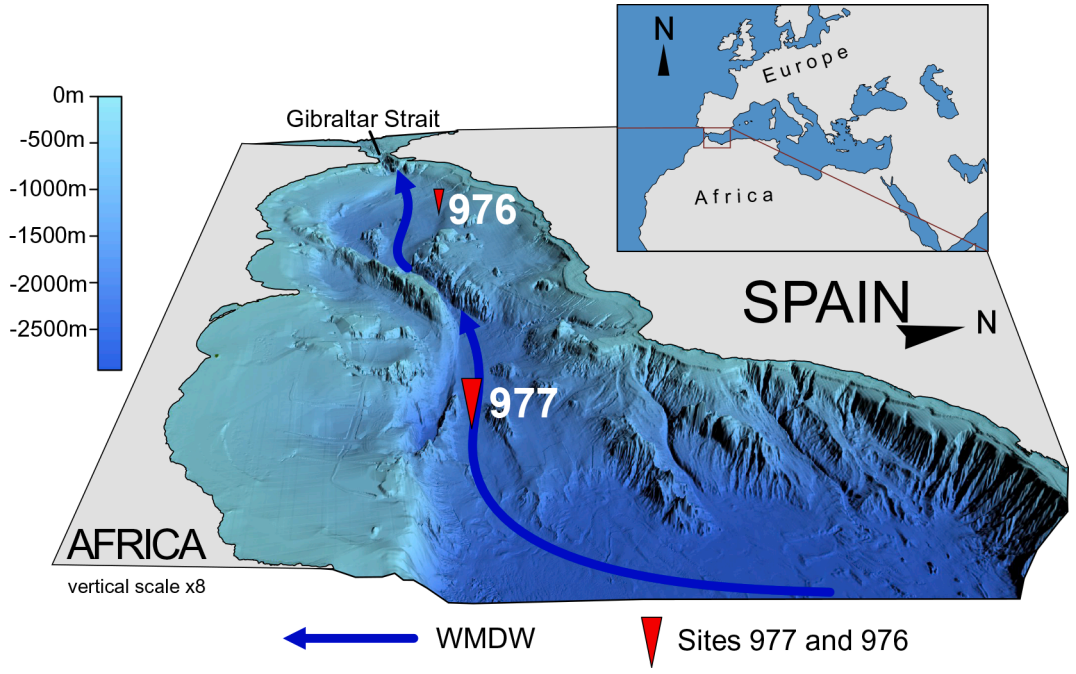

Fig. 1. Location of the ODP Sites used for the study (Sites 977 and 976). The blue arrow shows the main circulation pattern of the Western Mediterranean Deep Water towards the Gibraltar Strait (For interpretation of the references to colour in this figure legend, the reader is referred to the web version of this article).

2018; Pérez-Asensio et al., 2020).

One important open question surrounds the precise oxygen conditions during deposition. Ichnological analyses of deep-sea sediments have proven to be valuable for constraining oxygen conditions and OM preservation. At the time of deposition in deep-sea environments, depositional and ecological conditions at the sediment and in bottom waters —such as benthic food availability, oxygenation, hydrodynamic energy, and sedimentation rates— have a major impact on the macrobenthic trace maker community, hence on ichnological features as ichnodiversity, bioturbation degree and size of the traces, among others (i.e., Savrda and Bottjer, 1986, 1987, 1989, 2008; Savrda, 2007; Wetzel, 2010; Buatois and Mángano, 2011; Uchman and Wetzel, 2011, 2012; Wetzel and Uchman, 2012; Rodríguez-Tovar, 2021). For this reason, ichnological features are reliable proxies when reconstructing bottom- and pore-waters conditions and for palaeoceanographic interpretations (Löwemark et al., 2006; Löwemark, 2012; Rodríguez-Tovar and Dorador, 2015; Rodríguez-Tovar et al., 2015, 2018, 2019a, 2020a; Hodell et al., 2017; Sánchez Goñi et al., 2019). In the wake of a general ichnological study of sediment records from the Alboran Sea Basin, looking at the relationship between the abundance of bioturbation and climate changes during the Last Glacial Cycle (Casanova-Arenillas et al., 2020, 2021), the present study offers a detailed analysis of the westernmost ORLs distinguished over this time interval, so as to reconstruct palaeoceanographic dynamics. Our main aim is therefore to characterize the ORLs in terms of ichnology and sedimentology, beyond previous results, and typify ORLs based on such characterization. ORL types can then be related to variable palaeoenvironmental conditions, particularly oxygen content and ocean dynamics.

2. Regional setting

Over the decades, diverse studies explored ventilation and circulation in the Mediterranean using models, direct observations or proxies (e.g., Wüst, 1961; Millot, 1999; Pinardi and Masetti, 2000; Millot and Taupier-Letage, 2005; Sierro et al., 2005; Frigola et al., 2008; Rogerson et al., 2008; Naranjo et al., 2012; Pinardi et al., 2015; Bazzicalupo et al., 2018; Pérez-Asensio et al., 2020). The insights they provide for paleocirculation reconstructions have changed over time, from the early stationary models to current models based on dynamic changes and sub-basin switching circulation patterns. The general and simplified oceanographic setting of the water masses in the Mediterranean includes three masses that extend over the Eastern and Western Mediterranean, in turn, are divided into multiple sub-basins. Mediterranean circulation shows an anti-estuarine pattern (Millot, 1999; Millot and Taupier-Letage, 2005) with a less saline water mass —the Atlantic Water (AW)— entering through the Gibraltar Strait and circulating superficially, dominated by winds towards the Eastern Mediterranean. Then, when it reaches the eastern part of the Mediterranean, due to excessive evaporation in the Levantine Basin, it gains salinity and density; in conjunction with northern dry winds, it suffers cyclonic sinking, thereby generating the Levantine Intermediate Water (LIW) (Bethoux and Gentili, 1999; Millot and Taupier-Letage, 2005; Pinardi et al., 2015). The LIW circulates towards the west at middle depths and finally leaves the Mediterranean over the Gibraltar Strait, contributing to Atlantic circulation (Baringer and Price, 1999; Jiménez-Espejo et al., 2015; Naranjo et al., 2015). Two other water masses, the Western and Eastern Mediterranean Deep Water (WMDW and EMDW) flow in the deep parts of the two basins, resulting from the seasonal sinking of LIW and surface waters in the northern parts of the two sub-basins owing to open sea convention and cascading that is favoured by cold winds coming from the continent during winters (e.g., Medoc Group et al., 1970; Millot, 1999; Millot and Taupier-Letage, 2005; Schroeder et al., 2008, 2012; Durrieu de Madron et al., 2013; Naranjo et al., 2015; Somot et al., 2018; Cisneros et al., 2019). The WMDW, the water mass located at the bottom of the Western Mediterranean, is formed in the Gulf of Lions in winter by the above process of cyclonic sinking (e.g., Rhein, 1995) and is also important for Mediterranean outflow, mixing with the LIW and directly contributing by means of Bernuilli Aspiration (Rogerson et al., 2008; Millot, 2014).

The Alboran Sea Basin (Fig. 1), the westernmost Mediterranean Basin, it is of particular interest for palaeoenvironmental reconstructions for two reasons: 1) its high sedimentation rates allow for exceptional high-resolution studies of past oceanic conditions (e.g., Cacho et al., 2000, 2006; Martrat et al., 2007; Rodrigo-Gámiz et al., 2011, 2014; Martínez-Ruiz et al., 2015), and 2) its location between the Atlantic and the Mediterranean climate regimes, being influenced by both, and hence a key region for reconstructing the Atlantic influx and the Mediterranean Outflow as well as the Mediterranean water masses dynamics (e.g., Heburn and La Violette, 1990; Naranjo et al., 2015). The entry of AW through the Gibraltar Strait affects productivity in the Alboran Sea Basin, as the anticyclonic gyres and Atlantic Jet cause upwelling in the northern parts of the Basin (Sarhan, 2000). The Mediterranean water coming out from the Gibraltar Strait —the Mediterranean Outflow Water— influences the Atlantic overturning circulation, AMOC (Hernández-Molina et al., 2014; Bahr et al., 2015; Jiménez-Espejo et al., 2015). The Alboran Sea also receives the influence of water masses coming from the eastern basins, the LIW, and the WMDW.

The study sites are found at depths of 1984 and 1108 mbsl, under the influence of the WMDW (Bethoux et al., 1999). The varying conditions influencing deep water sinking in the northern sector of the basin may have influenced ORL deposition in this setting. Decreasing WMDW formation could have promoted dysoxic bottom waters over time, given that the dissolved oxygen in the Western Mediterranean Deep Water has been correlated (among other factors) to the deepwater removal influenced by climatic shifts (e.g., Rogerson et al., 2008; Mavropoulou et al., 2020).

The records studied entail an initial identification of ORLs and sediment characteristics established during ODP Leg 161. Afterwards, for many years, diverse work focused on the foraminiferal record and environmental and palaeoclimatological reconstructions have been published (e.g., Martrat et al., 2004, 2014; Pérez-Folgado et al., 2004; Combourieu Nebout et al., 2009). Notwithstanding, most of these studies focus on the Holocene and the most recent ORL. Research into the older ORLs is nearly absent and stands as a challenge for better understanding the origin of these organic-rich layers.

3. Materials and methods

The studied sediment record corresponds to the Sites 977 and 976 from Leg 161 of the ODP, and its general sedimentology and characteristics were described during the ODP cruise (i.e.,Shipboard Scientific Party, 1996a), and subsequent analyses strove to identify and define ORLs present in the record (Shipboard Scientific Party, 1996a, b; Murat, 1999). Both Sites are in the Alboran Sea Basin (Fig. 1): Site 977 deeper, at 1984 m, at the east of the Alboran Ridge; and Site 976 lies at 1108 m depth in the western Alboran Sea Basin. The sediments of the selected time interval (Last Glacial Cycle) correspond to open marine hemipelagic facies (Fig. 2) consisting of nannofossil-rich silty clay with an average clay content of 81% in Site 977 (Shipboard Scientific Party, 1996a) along with nannofossil rich clay, calcareous silty clay, and clay having 30–50% of carbonate content at Site 976 (Shipboard Scientific Party, 1996b).

The age models for these records were obtained from Martrat et al. (2004, 2014), and linear interpolation was used to correlate our depth data with age.

Ichnological analysis of the selected record was based on core images obtained from the ODP database. At Site 976, images were gathered from four available holes, drilled next to each other, so as to arrive at a more precise ichnological characterization (Fig. 2). Here, ichnological analysis entailed the application of high-resolution digital image treatment using Photoshop™ Software (Magwood and Ekdale, 1994;

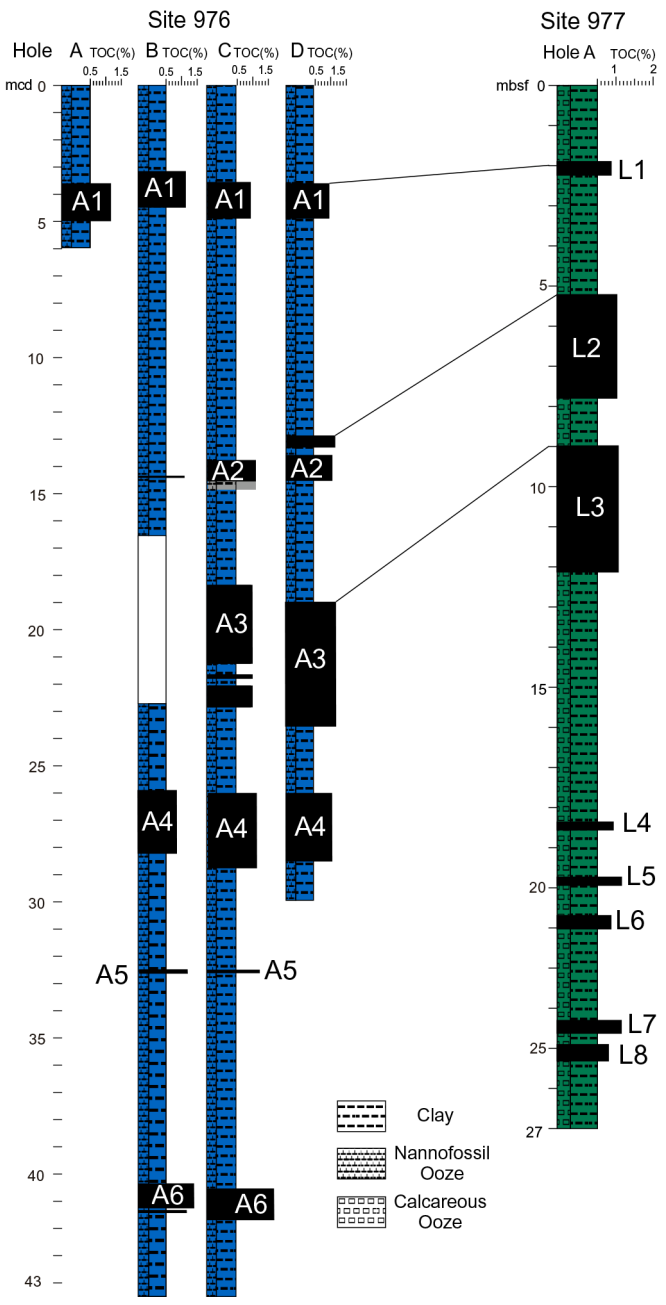

Fig. 2. General lithological logs of the studied holes from Sites 977 and 976 with the position of the ORLs (L1 to L8 in Site 977 and A1 to A6 in Site 976) and the corresponding TOC values (Shipboard Scientific Party, 1996a, b). In site 977 only one hole was drilled, the 977A. 4 holes that were drilled in Site 976 indicated from A to D.

Dorador and Rodríguez-Tovar, 2014a, 2014b, 2016, 2018; Rodríguez-Tovar and Dorador, 2014, 2015). This method increases the visibility of biogenic structures, providing for particularly successful results with modern sediment cores, where the visibility of the traces due to low lithification is very limited.

The main ORLs for ichnological analysis were distinguished according to the depths reported previously in ODP studies and published in the ODP Leg 161 Initial Reports (Shipboard Scientific Party, 1996a, b), being based on TOC values, magnetic susceptibility and colour.

A greyscale analysis was performed in view of average vertical grey values using ImageJ® software (e.g., Schindelin et al., 2012). The average grey value for the pixels in the horizontal lines of the images is obtained, after which a plot is made to represent the vertical grey value variation. Greyscale analysis has proven useful to visualize colour changes throughout sediment cores, and in particular, changes in reflectance. By identifying "darkness" and thus possible ORL intervals, these greyscale plots can mark the location of OM enriched intervals in the sediments. Several thin horizons along the cores were excluded from this study, since changes in grey values detected were at times due to artefacts such as variations in the position of the camera, or cracks and surface imperfections produced during the treatment of the core sections. The greyscale analysis was conducted only at Site 977. The available images from Site 976 were of comparatively poor quality —sediment colour is much more homogeneous than in Site 977, the only visible colour variations being a consequence of the incidence of light when photographed. Thus, the greyscale data served for a detailed analysis of the ORLs originally defined by the Shipboard Scientific Party, as well as for the addition of new ones.

4. Results

4.1. Greyscale analysis in Site 977

The grey value plot presents a pattern of clear variations that correlate well with the interval and the internal variation of the previously defined ORLs (Fig. 3). Yet it also shows variations not directly correlated with the ORLs identified on ODP Leg 161 (Shipboard Scientific Party, 1996a, b). Overall, the ORLs have a characteristic decrease in grey values (contrast of 20 to 30 points with respect to the surrounding sediment), especially L4, L5, L7 and L8. Internal variability is observed in L2 and L3, however, as well as in L1, which presents an extended range of variability, having a peak beyond the range of the layer as defined in the Initial Report.

During ODP Leg 161, at least 40 ORLs were described in the first 417 m of the holes drilled in the basin. At Site 977, eight of them are located in the upper 26 m corresponding to the Last Glacial Cycle. The obtained greyscale values improve the original ORL differentiation. Original ORLs (L1 to L8) were therefore characterized in greater detail, and new ORL intervals could be identified.

In view of the ORLs initially defined, the newly conducted analysis on ORL L1 reveals a grey value increase that extends further than the original interval (Shipboard Scientific Party, 1996a, b). The ORLs L4, L5, L7 and L8 (L6 is not visible) present a clear peak in grey value that is well-correlated with the darker laminated or bioturbated layers observed in the core images, supporting the original characterization (presented in Fig. 3).

In sum, the more recently conducted research allows for a tentative definition of new ORL intervals not considered in the original proposal based on fluctuations in greyscale values.

Accordingly, a total of seven new ORL intervals are defined here (a to g, blue colour bands, in Figs. 3), and previous ORLs, originally defined during ODP campaign, intervals have been modified, through extensions or subtractions (green and red colour bands, respectively, in Fig. 3). Moreover, ORLs L2 and L3 should be reconsidered, by the subtraction of some parts, as a possible succession of different events. The new colour bands are differentiated by contrast in the greyscale (reported contrast of between 12 and 24). The TOC values measured during the ODP campaign in the new layers go from 0.4% to 0.8%, below the established limit, but these data should be taken with caution and are of low resolution. The thickness of the new layers goes from 10 cm for layer a to 40 cm for layer g, for instance, the largest one observed.

4.2. Trace fossil assemblage

Trace fossil assemblages from the studied records at Sites 977 and 976 present a low-to-moderate diversity, consisting of *Chondrites*, *Planolites*, *Thalassinoides*, *Scolicia* and less frequent *Zoophycos* (Casanova-Arenillas et al., 2021) (Table 1). Concerning the ORLs intervals, *Chondrites*, *Planolites*, and *Scolicia* are the most abundant ichnotaxa.

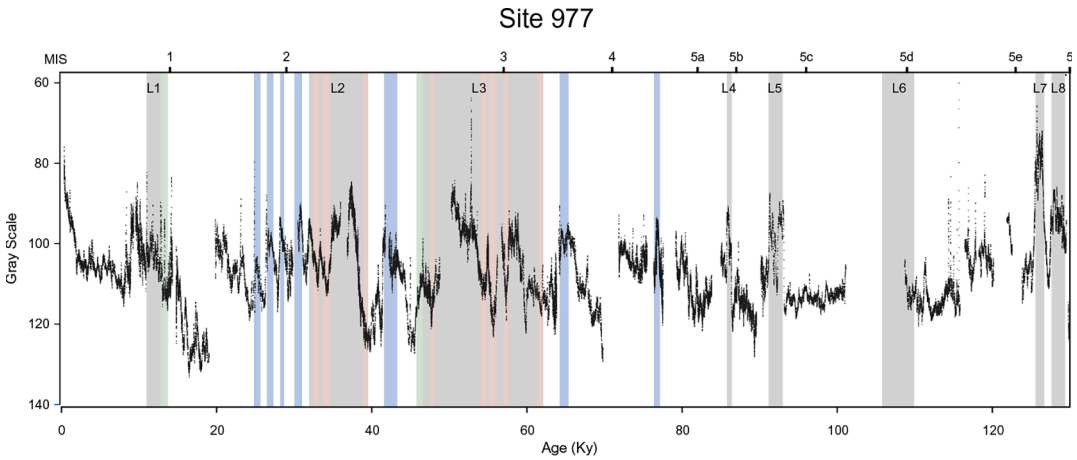

Fig. 3. Grey value plot in age with the location of the 8 ORLs (L1-L8) from site 977, hole A.

4.3. *Ichnological features in the organic-rich layers*

The ichnological analysis of the ORLs reveals significant variability mostly related to the presence/absence of traces, degree of bioturbation, ichnodiversity, and distribution.

4.3.1. *Bioturbation in the originally defined ORLs from Site 977*

The eight ORLs (L1 to L8) identified in Site 977 during ODP Leg 161 (Shipboard Scientific Party, 1996a, b) range from highly bioturbated to non-bioturbated and laminated sediments (Fig. 4; Table 2).

ORL L1 (~9 ka- ~14 ka) is about 30 cm thick, presenting a mottled background with locally identifiable discrete traces. The bottom of ORL L1 presents abundant bioturbation, in particular *Planolites*, *Scolicia* and *Thalassinoides*, and potential *Chondrites*. The size of the traces decreases upward. ORL L2 (~32 ka- ~39 ka) corresponds to a thicker interval of 220 cm. A mottled background is locally observed. The trace fossil assemblage consists of *Chondrites*, *Planolites*, *Scolicia* and *Thalassinoides* at the base. The abundance and size of biogenic structures are lower than in ORL L1, but also show a variable record throughout both ORLs, in association with colour variation in the sediment. ORL L3 (~46 ka- ~62 ka) is similar in thickness to ORL L2, around 310 cm, and shares the assemblage of *Chondrites*, *Planolites*, *Scolicia* and *Thalassinoides* at its base, but is less bioturbated. Like ORL L2, it shows variations in the trace fossil assemblage and the sediment colour through the ORL. In turn, ORL L4 (~85.5 ka- ~86.3 ka) is a thin layer, 30 cm, characterized by clear horizontal lamination and colour banding, and a generalized absence of bioturbation. Only occasionally in the lighter parts, small and disperse *Chondrites* can be tentatively identified. ORL L5 (~91 ka- ~93 ka) is 20 cm-thick, being very similar to ORL L4. ORL L6 (~105.8- ~110 ka) is between two core sections and its characteristics are not at all clear in the available images. ORL L7 (~125.5 ka- ~126.6 ka) is 25 cm-thick and resembles ORLs L5 and L4, except that at the top of this layer, a massive and sandy interval appears in which discrete traces attributable to *Planolites* of less than 1 cm can be observed. ORL L8 (~127.6 ka- ~129.3 ka) is a bioturbated layer, 40 cm-thick, very similar to ORL L1. The trace fossil assemblage consists of *Chondrites*, *Planolites*, and *Scolicia* with an upward increase in the trace size and bioturbation percentage.

4.3.2. *Bioturbation in the ORLs from Site 976*

The six ORLs (A1 to A6) from records at Site 976 differentiated during ODP Leg 161 (Shipboard Scientific Party, 1996a, b) are characterized by the presence of bioturbation and the absence of lamination (Fig. 5; Table 3). The ORLs from Site 976 present an incomplete chronostratigraphy and cannot be directly correlated in age or appearance with the ones from Site 977. Still, detailed characterization is interesting to discern lateral variations within the Basin and during ORL deposition.

ORL A1 has a similar appearance in the four drilled holes (Figs. 2 and 5), corresponding to a 90 cm bioturbated section and showing a mottled background. The trace fossil assemblage comprises *Chondrites*, *Planolites*, *Thalassinoides*, and *Scolicia*, the last especially abundant in the lower part. A decrease in the degree of bioturbation, abundance and size of trace fossils is observed upward. ORL A2 presents features similar to those of ORL A1, with *Chondrites*, *Planolites* and *Thalassinoides*, and *Scolicia* in the lower part. A reduction in size and abundance of the discrete traces is observed upward. Locally, a weak banding could be differentiated in the middle part, associated with the darker sediments. ORL A3 appears as a long, 320 cm, not always well-preserved layer. Bioturbation is moderate, with local increases in abundance in the middle and upper parts. Some darker intervals lack trace fossils, but banding/lamination is likewise absent. The trace fossil assemblage mainly comprises *Chondrites*, *Planolites* and *Thalassinoides*, with occasional *Scolicia*. Tentatively, some structures could be assigned to *Zoophycos*. ORL A4 refers to a 150–170 cm thick section with low and sparsely distributed bioturbation, though higher abundance is noted upward. The trace fossil assemblage consists of *Chondrites*, *Planolites* and *Thalassinoides*, with *Scolicia* mainly in the upper part. Tentatively, like in ORL A3, some structure(s) could be assigned to *Zoophycos*. ORL A5 is a thin, 2 to 10 cm thick, bioturbated layer with *Chondrites* and *Planolites*, and probably *Scolicia*. Locally, weak banding is envisaged. +ORL+ A6 +, about 60–70 cm thick, is moderately bioturbated, with an assemblage of *Chondrites*, *Planolites*, *Scolicia* and *Thalassinoides*.

4.4. *Ichnological and sedimentological features: Types of ORLs*

Ichnological (ichnotaxonomy, distribution, size, and abundance of the traces) and sedimentological features —including the thickness of the ORL intervals and grey values in the studied records— allowed us to characterize different ORL types beyond the ones originally described at Sites 976 and 977 (Shipboard Scientific Party, 1996a, 1996b). Differentiation was more feasible for Site 977, as the images and data were more detailed, whereas for Site 976 merely general discernment was attempted. Only the originally described ORLs from ODP are included in this analysis to detail palaeoenvironmental interpretations previously proposed. The differentiated types are as follows (Fig. 6):

Type 1: Characterized by a thickness ranging from 30 to 40 cm in Site 977 and up to 120 cm in 976. Bioturbation is generalized, with the presence of a mottled background, and with trace fossils registered throughout the entire ORL, but showing differences from bottom to top. At the base, burrows are abundant and range from 5 cm to a few millimetres. The size and abundance gradually decrease upward. Trace fossil assemblage consists of abundant *Scolicia* and *Planolites*, frequent *Chondrites*, and possible *Thalassinoides* in the base. ORL L1 and ORL L8 of

Table 1
Different ichnogenus differentiated.

Ichnogenus	Ichnological features	Relationship with ORL intervals	Interpretations	References
Chondrites	A cluster of millimetric size circular to ovalate burrows	Disseminated, low abundance. Can crosscut other traces	Deep tier structure. Feeding activities of chemo-symbiotic organisms. Tolerant to low oxygen conditions	von Sternberg (1833), Hertweck et al. (2007), Rodríguez-Tovar et al. (2009); Rodríguez-Tovar and Uchman (2011), Bromley (2012), Knaust (2017), Baucon et al. (2020)
Planolites	Circular to subcircular small burrows (less than 0.5 cm). Fill colour different from that of the host sediment	Mainly registered at bottom or top in ORLs, showing multiple changes in colour and bioturbation. Occasionally in the middle parts for unchanged ORLs	Produced by active deposit feeders, usually attributed to worm-like organisms, though other means of production like molluscs and arthropods cannot be discarded	Nicholson (1873), Pemberton and Frey (1982), Keighley and Pickerill (1995), Rodríguez-Tovar et al. (2009)
Thalassinoides	Large burrows, of over 1 cm in diameter. Fill darker than the surrounding sediment.	At bottom and top of the ORL intervals in both cores, and rarely in the middle part	Middle-tier structure representing the action of organisms inhabiting galleries for dwelling and feeding activities at few centimetres below the sediment surface. The producer is usually interpreted as a crustacean, particularly the callasinoids	Ehrenberg (1944), Frey et al. (1984), Nickell and Atkinson (1995), Schlirf (2000), Ekdale and Bromley (2003), Knaust (2017)
Scolicia	Large burrows, usually exceeding 1 cm, showing a cross-section where a small dot of darker sediment appears in the centre of a lighter subcircular burrow, or as a lamellar filled structure representing the displacement of the producer	This trace has been identified in several parts of the ORLs, determining significant bioturbation	Produced by deposit-feeding echinoids and can be found in silt-sized sediments. Its presence is associated with the abundance and quality of benthic food	Quatrefages (1849), Wetzel (1991, 2008), Carmona et al. (2020)
Zoophycos	Horizontal spreiten burrows darker than the surrounding sediment.	Scarce, only registered at the top of some ORLs from core 976.	Unknown producer, being assigned to variable behaviour but mainly to feeding activities.	Massalongo (1855), Bromley et al. (1999), Rodríguez-Tovar et al. (2009) Hunter et al. (2012)Löwemark (2012); Kotake (2014), Löwemark (2015), Dorador et al. (2016), Łaska et al. (2017)

Site 977 (Table 2), and ORLs A1, A2 and A6 from Site 976 (Table 3) are assigned to this type.

Type 2: Characterized by thick intervals, up to 310 cm, and cyclic changes in colour and bioturbation features, as well as a clear greyscale internal fluctuation. In Site 977, they correspond to the ORLs L2 and L3 (Table 2), and in Site 976, they could be assigned to the ORLs A3 and A4 (Table 3). Given their thickness and features, an evident differentiation from other parts of the cores, not associated with ORLs, is unclear. Even though a transition from non-ORL bioturbated sediment with big traces to an ORL having unbioturbated or low-bioturbated sediments is recognized. Type 2 also includes heavily to moderately bioturbated intervals.

Type 3: It is characterized by well-developed laminations and absence of bioturbation, as well as an evident peak in the inverted greyscale, and magnetic susceptibility reduction, determining a good differentiation from the surrounding sediments. This type is assigned to ORLs L4, L5 and L7 of Site 977, corresponding to intervals about 20 to 30 cm thick, registered from the end of the penultimate glacial maximum to present (Table 2). It cannot be discarded that ORL L6 could also correspond to type 3, but the location between two coring sections makes a conclusive assignation difficult. At Site 976, these laminated ORLs are not present (Table 3).

5. Discussion

During ODP Leg 161, other than the classical definition of ORLs based on TOC values (Murat, 1999), the shipboard party relied on further characteristics, e.g., colour and magnetic susceptibility. In the Alboran Sea Basin, significantly higher sedimentation rates than in the eastern basins led to dilution and lower TOC content in ORLs and higher background values. Thus, the ORL definition was based on a 0.8% minimum TOC together with colour contrast and magnetic susceptibility (Murat, 1999). In addition to this, as mentioned, the greyscale was used to extend information based on the observed ichnological features, even though not all the original ORLs present a clear differentiation when the core surface is observed.

5.1. *Ichnological features in the ORLs and environmental implications: The role of anoxia*

In general, the ichnological information has proven to be a very useful proxy for the characterization of past anoxic events as the Faraoni Event (upper Hauterivian; Rodríguez-Tovar and Uchman, 2017), the Bonarelli Event (Cenomanian-Turonian boundary; Uchman et al., 2008, 2013a, 2013b; Rodríguez-Tovar et al., 2009, 2020b; Rodríguez-Tovar and Uchman, 2011; Monaco et al., 2012, 2016) and the Toarcian Oceanic Anoxic Event (Early Toarcian; i.e., Rodríguez-Tovar and Uchman, 2010; Reolid et al., 2014; Miguez-Salas et al., 2017, 2018; Rodríguez-Tovar et al., 2017, 2019b). For further information, see the recent review on the Toarcian Oceanic Anoxic Event revealing the variable oxygenation and the absence of global and generalized anoxia (Rodríguez-Tovar, 2021).

The ichnological characteristics of more recent sediments such as the ORLs have been poorly studied, however. Scarce and undetailed references to bioturbation were originally included in ORLs descriptions in the ODP Leg 161 Initial Reports (Shipboard Scientific Party, 1996b), and just recently more detailed ichnological analyses were undertaken (Pérez-Asensio et al., 2020).

The occurrence of ORLs involves complex processes that may depend on such factors as primary productivity, anoxic conditions, and sedimentation rate, which play a variable role according to different authors (Müller and Suess, 1979; Pedersen and Calvert, 1990; Kuypers et al., 2002; Rohling et al., 2015). Again, not only the increase in the OM flux is determinant for the formation of these layers; in fact, oxygen restriction without enhanced productivity might not result in ORLs deposition (Rogerson et al., 2008).

According to the obtained data, some of the ORLs registered during the Last Glacial Cycle in the Alboran Sea Basin at Sites 977 and 966 support dysoxic (2.0–0.2 ml/l O_2) to suboxic (0.2–0.0 ml/l O_2) and anoxic conditions (0.0 ml/l O_2), following values from Tyson and

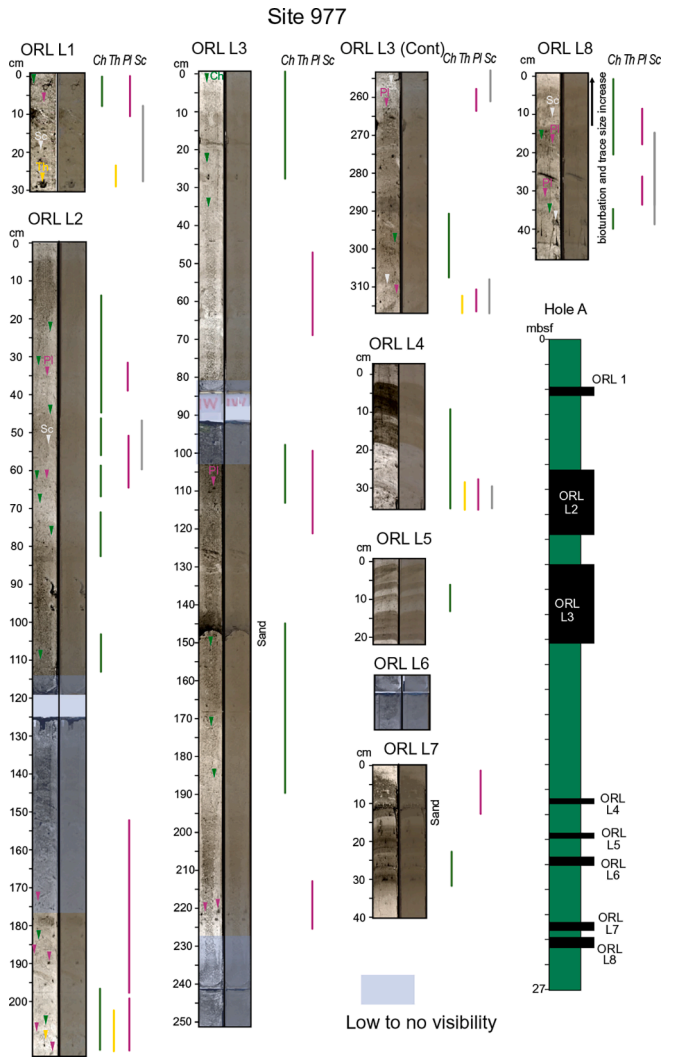

Fig. 4. ORLs differentiated in Site 977 with the indication of the trace fossil distribution. *Ch* = *Chondrites*,*Pl* = *Planolites*, *Sc* = *Scolicia*,*Th* = *Thalassinoides*.

Pearson (1991), as indicated by variability in the ichnological features and the local presence of lamination.

In oxic conditions with a steady flux of benthic food, light sediments (corresponding to non-ORLs) with TOC values below 0.8% are observed, and a well-developed trace maker community determines a variable number of discrete traces imposed upon a mottled background (Fig. 7A). The ichnological assemblage associated with such conditions features the presence of more or less abundant *Thalassinoides* and *Planolites*, with punctual *Scolicia* and *Zoophycos*. Oxygen levels are maintained above the dysoxic threshold with certain fluctuations, which produced the variations evident in the trace fossil assemblage and abundance.

During deposition of the Type 1 ORL, generalized dysoxic conditions with abundant benthic food gave rise to discrete traces, and a mottled background, in combination with darkly coloured sediments and high TOC values of 0.8 to 1.2% (Fig. 7B). Dysoxic conditions impeded a well-developed trace maker community. Upward, decreases in both abundance and size of biogenic structures reveal the deterioration of palaeoenvironmental conditions during ORL deposition. In Type 2 ORL, variations in colour, TOC, and trace fossil assemblage are observed, with lighter sediment presenting moderately abundant traces and darker intervals presenting low or absent bioturbation. This suggests variable oxygen conditions during the ORL deposition, from moderately to extremely dysoxic (Fig. 7C).

Type 3 ORL corresponds to laminated and non-bioturbated short intervals, indicating an inhabitable macrobenthic environment. The absence of a macrobenthic tracemaker community supports suboxic or anoxic conditions (Fig. 7D).

According to the above, even though ORLs have been commonly related with periods of deep-water stagnation and oxygen depletion (e.g., Rogerson et al., 2008; Rohling et al., 2015; Pérez-Asensio et al., 2020), and largely associated with laminated, non-bioturbated, or only scarcely bioturbated sediments, our results are indicative of significant variability in palaeoenvironmental conditions. All the originally proposed ORLs at Site 976 and most of those at Site 977 —corresponding to ORLs types 1 and 2— are bioturbated, including a mottled background and discrete traces. This fact supports the absence of generalized anoxic conditions during some of the ORL intervals in the Alboran Sea Basin, but rather oxygenated conditions favouring the development of a macrobenthic trace maker community and, in turn, bioturbation. Only ORLs assigned to Type 3, showing lamination and absence/scarce bioturbation, could be indicative of such anoxic conditions.

5.2. ORL position, fact or artefact?

Traditionally ORLs are defined by increased TOC values with respect to surrounding sediments. Nonetheless, post-depositional modifications can lead to a drop in TOC percentages —the presence of "ghost" layers only detectable by geochemical data, as observed in other basins (Jung et al., 1997; Larrasoaña et al., 2006; Löwemark et al., 2006). Thus, colour and ichnological information evidencing variations in oxygen conditions even when TOC enrichment has been lost could be used to recognize ORL intervals irrespective of TOC values. Based on this possibility, we tentatively propose the existence of new intervals, including some that could have TOC contents below the 0.8% TOC threshold.

In Fig. 8 these new intervals are presented, including some images that serve to visualize variations in the core surface. The intervals are thin and tend to correlate with the fluctuations observed in the [Ca^{+2}] plot and the Sea Surface Temperature (SST) (Fig. 8). Such good correlation evidences that colour variations respond to climate changes taking place in the Northern Hemisphere and over the Alboran Sea.

As mentioned before, in addition to the new ORL intervals proposed, some of the original ORLs have been modified by extensions or subtractions of certain parts. One clear example is ORL1, profusely studied, with a well-known position and age. According to the greyscale analysis, its position respect to the ODP initial reports must be modified, by extension in the lower part, suggesting that this layer is probably thicker than originally indicated. This proposal is concordant with the age obtained in studies of the ORL1 in other records in the Mediterranean Sea (Cacho et al., 2002; Rogerson et al., 2008; Rodrigo-Gámiz et al., 2011; Martínez-Ruiz et al., 2015). Furthermore, the extension is in consonance with proposed ages of ORL L1 in the Alboran Sea (Jiménez-Espejo et al., 2015; Pérez-Asensio et al., 2020), since when converting the depth data to age using the Martrat et al. (2004) age model, the ORL L1 extends from 14 ka to 8 ka. The opposite occurs with ORLs L2 and L3, where colour changes might evidence an overestimation of the thickness of ORL L2 and L3 originally considered.

According to the above, the originally proposed ORL position, number, thickness and age in the Alboran Sea Basin could be different in some cases. Variations in the colour and ichnological features within thicker ORLs could, moreover, be indicative of changes in palaeoenvironmental conditions during the ORLs deposition, revealing interruptions during ORL deposition or the existence of multiple shorter ORL events that were combined in the original description.

5.3. Palaeoenvironmental and palaeoceanographic implications

It must be stressed that ORLs cannot be correlated with the eastern sapropels (Rohling et al., 2015): a major difference, apart from lower carbon content, resides in chronology, since ORLs were not always deposited during the same time intervals. As stated by Rogerson et al.

Table 2
ORLs defined by the ODP scientific time in Site 977. Type as defined in this paper, sedimentary features, ichnological features", grey values and TOC measurements from the Initial Reports.

ORL	Type	Sedimentary features	Ichnological features	grey values	TOC
977					
L1	Type 1	30 to 40 cm sections with no sedimentary structures	Abundant *Scolicia* and presence of *Planolites*, *Chondrites* and *Thalassinoides* at the base of the layer. The size and abundance of the traces decrease from bottom to top of the section	105–95	0.87
L2	Type 2	220 cm section with high cyclical variability in colour	Highly bioturbated in the base with *Thalassinoides*, *Planolites* and *Chondrites*. A gradual decrease in size and abundance of the discrete traces	113–88	1.02 to 0.79
L3	Type 2	310 cm section with cyclical variability in colour and sedimentological features. Higher values in greyscale towards the top of the section	Bioturbated in the base with *Chondrites*, *Thalassinoides* and *Scolicia*	123–87	1.07 to 0.87
L4	Type 3	30 cm short section with lamination and two greyscale levels, higher values in the top middle section	Low bioturbated to no-bioturbated, with only *Chondrites* as a possible discrete trace. Abrupt decrease of bioturbation at the beginning of the ORL	119–106	0.93
L5	Type 3	20 cm short section with lamination. Abrupt changes in the greyscale values alternating between darker and lighter sediments	Low to no-bioturbated, with only *Chondrites* as possible discrete trace	115–110	1.13
L6	Type 3*	Not studied in detail due to core limitations		116–92*	0.79
L7	Type 3	40 cm laminated section, with alternating changes in greyscale value. The top presents a sand intrusion followed by non-laminated sediment	From the base to the sand intrusion, no to low bioturbation with only *Chondrites* as a possible trace. The top of the layer presents a dark coloured interval with abundant *Planolites*	90–72	0.98,1.13
L8	Type 1	40 cm section with no lamination. Greyscale variations with two intervals, with lighter sediment in the base	Abundant *Scolicia*, presence of *Planolites* and *Chondrites*. Abundance and size of the *Scolicia* higher in the top of the layer, making the colour of the sediment lighter	103–86	1.00, 1.26

(2008), ORLs do not occur during pluvial maxima every time; and the origin cannot, therefore, be directly related to the irruption of freshwater. In the Eastern Mediterranean sapropel origin is described as a result of an increase in precipitation and subsequent freshening of the surface layer that produces buoyancy increase and deep-water stagnation, in combination with productivity blooms produced by the nutrients reaching the sea within the rivers (Rohling et al., 2015). It is possible, however, that the irruption of freshwater from continental ice not coincident with pluvial maximum, especially from the Alps, could induce the buoyancy increase decoupled from pluvial maxima during deglaciation events (Rogerson et al., 2008).

Recent works, focused on the same ODP Sites from the Alboran Sea Basin, demonstrate that there is a correlation between the ichnological features variations and palaeoceanographic conditions, especially in terms of changes in ventilation and benthic food availability (Casanova-Arenillas et al., 2021). Thus, the integration of ichnological information with other sedimentological characteristics is one key for understanding the palaeoenvironment associated with the different types of ORLs over the Last Glacial Cycle. The occurrence of the ORLs —whether previously defined or tentatively proposed here— is coherent with restricted ventilation during some of the warming periods over the last interglacial, and at least partial oxygenation occurring between these depositional events (Fig. 8). The significance of these restriction events in combination with factors including the LIW characteristics could have led to the differences among the different ORLs, or even stand as the main cause behind these differences, as LIW composition can affect the sinking and composition of the WMDW (Incarbona and Sprovieri, 2020). Notably, during Heinrich events, low saline water coming from the polar iceberg melting entered through the Gibraltar Strait, impacting circulation in the Mediterranean (Cacho et al., 2002; Sierro et al., 2005), notwithstanding, it did not produce substantial deep-water restriction (Sierro et al., 2005), which is coherent with the apparent absence of any relation between the Heinrich events and either the greyscale of the bioturbational features in the studied record. Over the Last Glacial Cycle, intense variation in atmospheric conditions resulted in rapid changes in climate conditions over the Western Mediterranean (Martrat et al., 2004; Bazzicalupo et al., 2018), hence in the atmosphere/ocean dynamics, affecting deep-water masses and their ventilation (Cacho et al., 2002). In particular, the last glacial maximum is associated with cold and arid conditions (Lionello, 2012) that affected oceanographic conditions driving ORL formation. Still, the correlation of ORLs with climate events is not fully understood. Comparison of the three differentiated types of ORLs at Site 977 with the SST record (Martrat et al., 2004) in conjunction with the use of calcium ion concentration data ($[Ca^{2+}]$) for better visualization of the stadial/interstadial variation in the northern hemisphere (Rasmussen et al., 2014), and the magnetic susceptibility and TOC contents (Shipboard Scientific Party, 1996b), would evidence diverse environmental conditions for these ORL types (Fig. 8). Meanwhile, $[Ca^{2+}]$ in the ice cores is an excellent proxy for stadial in the northern hemisphere, as it records the dust concentration, which is indicative of changes in regional and hemispheric circulation (Fischer et al., 2007, Rasmussen et al., 2014).

Type 1, as the most bioturbated one, appears in both Terminations I and II (TI and TII), in agreement with the onset of warmer conditions and thus less deep-water sinking. Type 1, taking in ORL L1 from Site 977 and probably A1 from Site 976, is defined as the basin-wide ORL1 (Rogerson et al., 2008; Pérez-Asensio et al., 2020). Under Type 1 the ORL L8 can also be included, having formed towards the end of the penultimate glacial period warming phase, and having ended following the interglacial post-glacial warm period. As type 1 ORLs presents abundant bioturbation, it can be interpreted as revealing generalized oxic/dysoxic conditions that occurred at least partially during parts of the deposition of this layer. Therefore, extended suboxic/anoxic conditions were not reached during the TI and TII in this Basin, and the dysoxic conditions were not constant. ORL type 1 is accordingly suggested to be mostly related to productivity variations rather than to a strictly anoxic environment. The fact that both type 1 ORLs (ORLs L1 and L8) appear during a similar climatic trend, at the beginning of Terminations I and II (Fig. 8), further supports the idea that similar events occurred at the end of the penultimate and last glacial periods, even though the two deglaciations show differences —for example, the absence of a cold spell like the younger dryads in the TII (Martrat et al., 2014). A similar ORL appearing in the deglaciation event might signal enhanced productivity events with no strong deep-water restriction,

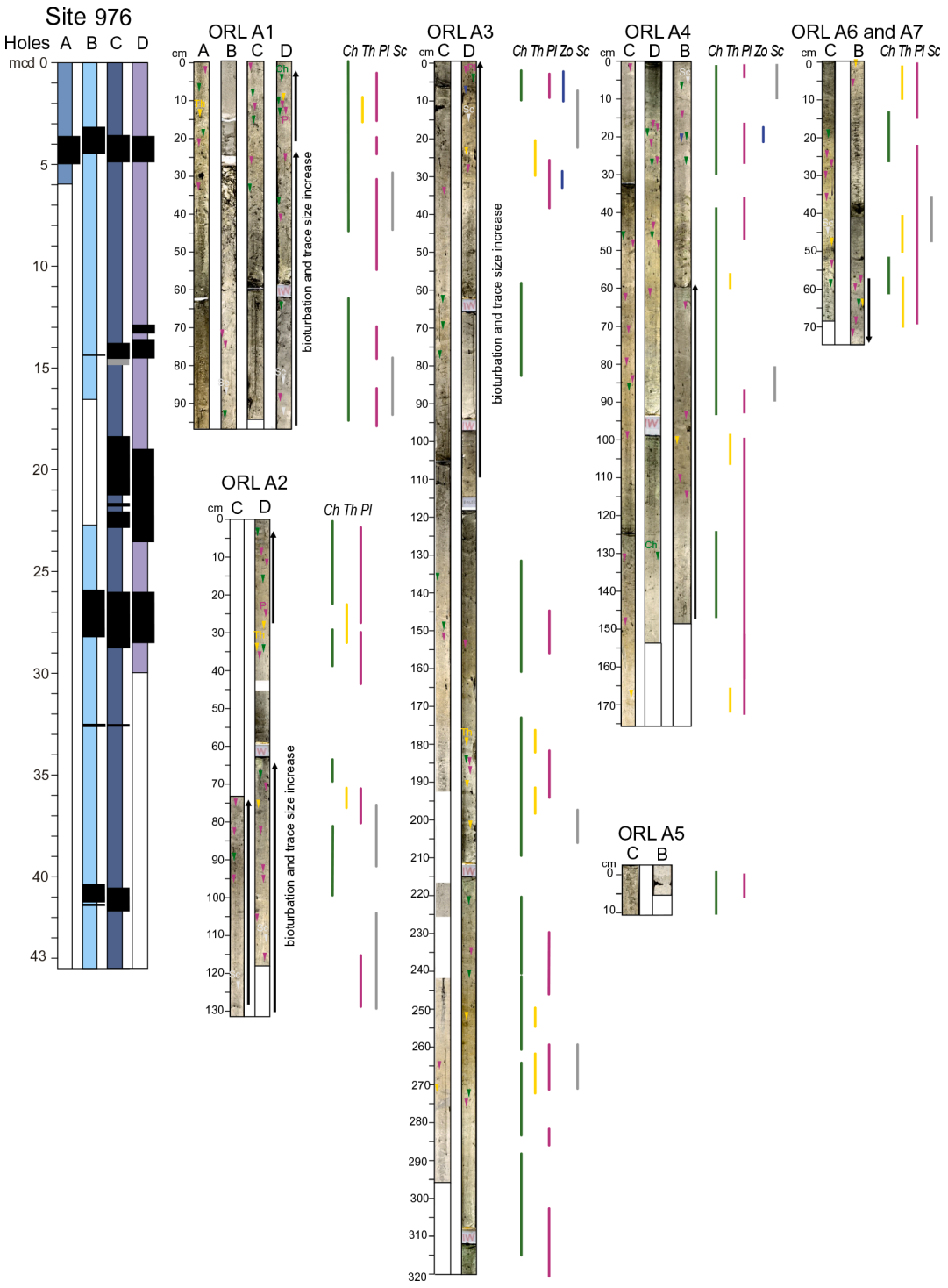

Fig. 5. ORLs differentiated in Site 976 with the indication of the trace fossil distribution. *Ch* = *Chondrites*, *Pl* = *Planolites*, *Sc* = *Scolicia*, *Th* = *Thalassinoides*. The 4 holes that were drilled in Site 976 are indicated from A to D.

allowing for a diverse trace maker community. At the end of the Last Glacial Period, enhanced primary productivity has been linked to Atlantic inflow in the Alboran Basin because of the wind and jet induced upwellings (Ausín et al., 2015a, 2015b) during the end terminations and Younger Dryas; a similar context could be envisaged for the TII.

Type 2, including thicker ORL intervals with internal cyclic changes in bioturbation and colour than when plotted with SST and [Ca^{+2}], shows a correlation with the —D-O interstadial-stadial cycles. Assuming a direct correlation between the climate changes in the Mediterranean and the deep-sea bottom conditions (e.g., Martrat et al., 2004; Frigola et al., 2008), these cyclic variations suggest oxygenation changes throughout the entire Alboran Basin during the period of deposition of these thicker layers.

Type 3 ORL correlates with warm periods, except for ORL L4, which is associated with a cold phase. Type 3 is interpreted to be related to suboxic/anoxic conditions based on the absence of bioturbation and a well-developed lamination. When considering climate conditions, the relation to warming phases is recognized but points to highly variable correlation; at different phases of a warm interstadial, at the beginning and the end of the warming phase, and at the peak of the interstadial

Table 3
ORLs defined by the ODP scientific time in Site 976. Type as defined in this paper, sedimentary features, ichnological features and TOC measurements from the Initial Reports.

ORL	Type	Sedimentary features	Ichnological features	TOC
976				
A1	Type 1	100 cm layer without identifiable sedimentary structures	Highly bioturbated with *Chondrites*, *Planolites* and *Thalassinoides*.*Scolicia* is abundant in the base and probably present in the middle part of the interval. Burrow sizes increase from the bottom to the middle (30 cm) and then decrease to the top	1.13. 0.8, 0.95, 0.93
A2	Type 1	110 to 50 cm layer without identifiable sedimentary structures. A colour change appears, with lighter sediment at the base and darker to the top	Presence of *Scolicia* in the base. *Chondrites*, *Planolites* and *Thalassinoides* can be identified in the rest of the interval. The abundance and size of the burrows increase from the bottom to the top of the layer (especially seen in hole C), with a decrease from the middle part (60 cm) in hole D	1.09, 1.1,
A3	Type 2	A long section of up to 320 cm. Variation in grey value with several colour cycles	Presence of*Chondrites*, *Planolites* and *Thalassinoides* in the bottom, middle and top of the section. *Zoophycos* appears at the top of the layer. The size and abundance of the burrows are low, increasing in the middle (190–210 cm) and top of the ORL section	0.97, 1.08, 0.75, 0.560
A4	Type 2	Length up to 170 cm in section without identifiable sedimentary structures	Presence of *Chondrites*, *Planolites* and *Thalassinoides*. Increase in size and abundance of burrows from bottom to 50 cm, and then decrease to the top. Possible presence of *Scolicia* in the middle and top of the layer. *Zoophycos* in the top	0.82, 1.1, 0.97,0.92, 1.01
A5	–	Short 10–5 cm layer with no structures	Highly bioturbated with *Chondrites* and *Planolites*	1.19,
A6	Type 1	50–60 cm long with greyscale variations from dark to lighter sediment	*Chondrites*, *Planolites* and *Thalassinoides*. *Scolicia* over the beginning of the layer. The trace size and abundance decrease from the bottom to the top of the layer	1.42, 1.85

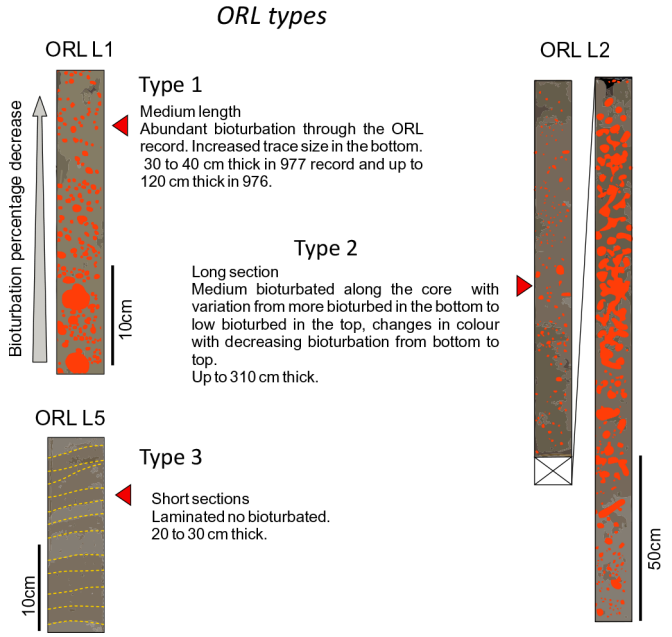

Fig. 6. Examples of differentiated ORL types with description and schematization.

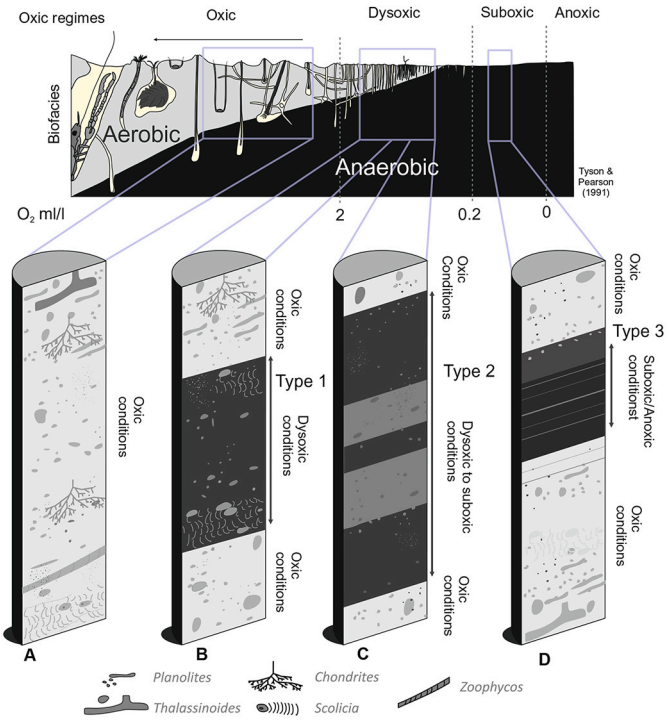

Fig. 7. Top: Schematization of the oxic regimes and tiering according to Tyson and Pearson (1991). Bottom: Scenarios for oxygen conditions according to the ORL types proposed (see text for explanation).

(Fig. 8). Interestingly, some of the Type 3 ORL ages coincide with the low $\delta^{18}O$ values in Soreq cave speleothems (Bar-Matthews et al., 2000) from the Eastern Mediterranean related to sapropel formation: ORL L4 (~85.5- ~86.3 ka) could match low $\delta^{18}O$ (~85- ~ 79 ka) related to S3 formation (83 ka; Rossignol-Strick and Paterne, 1999), while ORL L7 (~125.5- ~126.6 ka) fits with the low $\delta^{18}O$ (~124- ~ 119 ka) related to S5 formation (124.2 ± 2 ka; Rossignol-Strick and Paterne, 1999). Even though we cannot assign a type to ORL L6, due to visibility issues, it is dated at ~105.8- ~110 ka, and could coincide with the $\delta^{18}O$ (~108- ~ 100 ka) related to S4 (103.3 ± 3.4 ka, Rossignol-Strick and Paterne, 1999). This means that not all the ORLs are decoupled from the sapropel events in the East, and that the conditions producing sapropels likewise bear an impact on ORL formation at certain points of the geological record, and interestingly this coincidence is with the best defined, bioturbation lacking, suboxic/anoxic ORLs from the Alboran Sea Basin.

Considering the subtractions and additions of the Original ORLs (Fig. 8) and the new, tentatively defined ORLs (a, b, d, e, f, g in Fig. 8), a clear coincidence can be seen in many cases with the climatic variations of the northern hemisphere. The fact that some of them appear in the middle of warm periods or during warming phases agrees with the theoretical model of deep-water renewal being controlled by winter's cold north winds, and to the entry of freshwater from continental ice

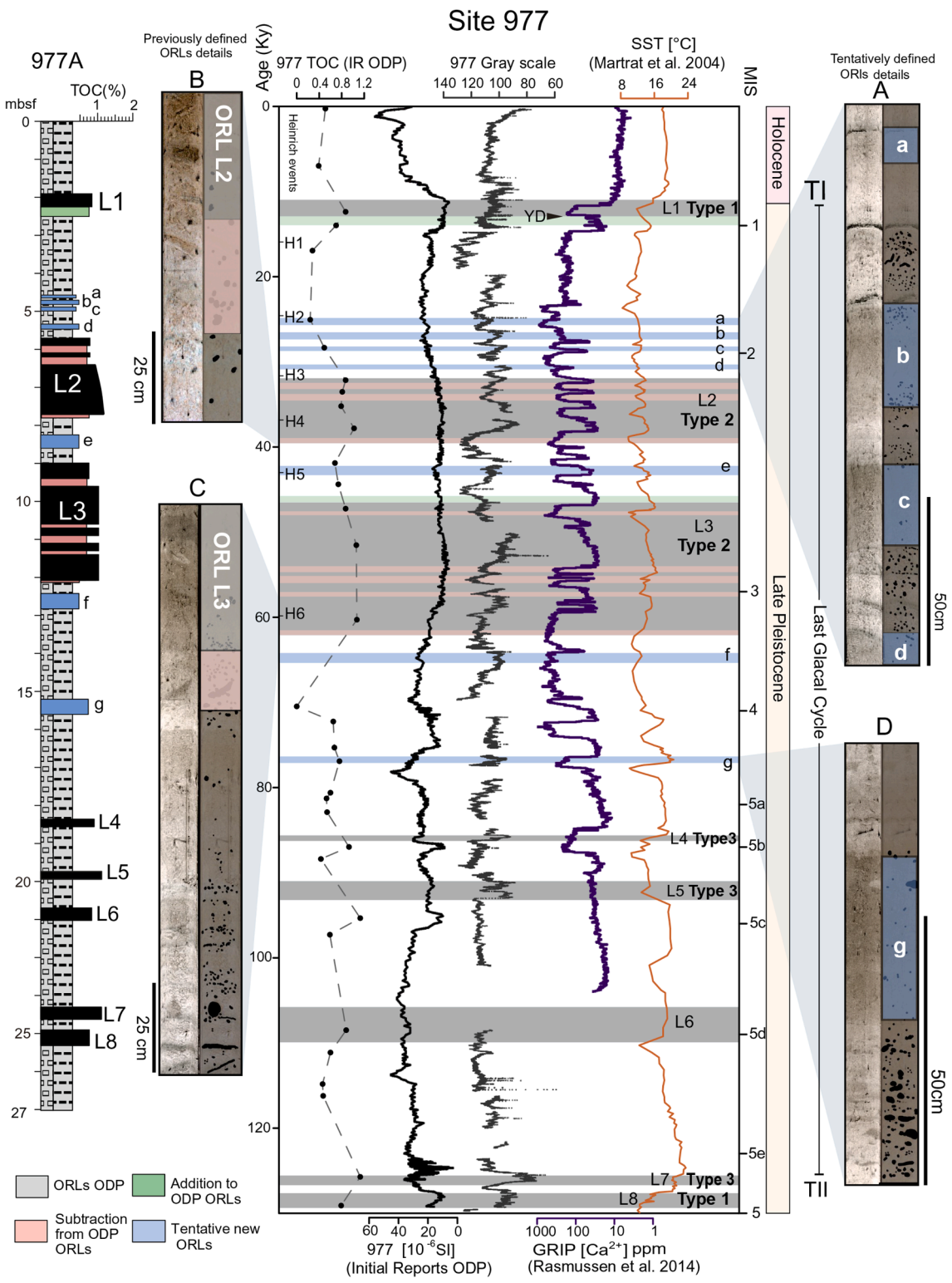

Fig. 8. Correlation between the greyscale and colour values, TOC, magnetic susceptibility, and sea surface temperature (SST) for Site 977. The position of the ORLs is indicated, with differentiation between the original proposal from the initial reports (grey), the added parts (green) and the removed parts (red), and the new defined ORLs (a to g; blue). MIS: Marine Isotope Stage. The 6 Heinrich Events are indicated in the left part of the figure. In addition, 4 details of the core surface of both new defined ORLs and changes in the previously defined ORLs are added indicated with the letters A, B, C and D. [Ca^{+2}] here is a proxy for stadial in the northern hemisphere, as it records the dust concentration over Greenland, indicative of changes in regional and hemispheric circulation changes. (For interpretation of the references to colour in this figure legend, the reader is referred to the web version of this article.)

melting; altogether, they induce buoyancy changes that inhibit water sinking, and imply reduced Bernoulli Ventilation due to sea level increase (Cacho et al., 2002; Frigola et al., 2008; Rogerson et al., 2008). This correlation supports the connection of the deep environments in the Western Mediterranean with the Westerlies and the AMOC variations during climatic changes. Such a correlation is not always observed, however, and some ORLs (newly or previously defined) may not appear during warming phases or might even be coincident with minimum SST values (e.g., ORLs "a", or "L1" Fig. 8). In sum, there is a complicate combination of multiple factors controlling the events, not producing an always coincident response to the same climatic variations, implying there is a need for a much further exploration of the different ORLs of the Mediterranean, beyond the ORL1, and extending to previous glacial cycles.

6. Conclusions

A detailed sedimentological and ichnological analysis of the ORLs deposited over the Last Glacial Cycle in the Alboran Sea Basin and recorded at ODP Sites 977 and 976, reveals the presence of different types of ORLs, and supports variable environmental conditions over this time interval resulting in ORL deposition. Three ORL types (1, 2 and 3) are recognized according to variable palaeoenvironmental parameters, and main variations in oxygen conditions. Type 1, with an intermediate thickness (30 to 40 cm), corresponds to high to moderate bioturbated intervals. The trace fossil assemblage consists of abundant *Scolicia* and *Planolites*, frequent *Chondrites*, and possible *Thalassinoides* in the base, supporting dysoxic conditions during deposition, which prevented a well-developed trace maker community. Type 2 corresponds to thicker intervals (up to 310 cm), showing an alternance of highly to moderately bioturbated intervals, revealing variable oxygen conditions from moderate to extremely dysoxic or even suboxic ones. Type 3 consists of thin (20 to 30 cm), laminated intervals characterized by an absence of bioturbation, indicating anoxic or suboxic conditions and determining an unfavourable macrobenthic habitat.

Ichnological and colour analyses made it possible to refine the original ORLs characterization, by adding new ones, or extending or subtracting parts of the initially described ORLs. Seven new intervals have been tentatively added (a, b, c, d, e, f, g) to the originally proposed ORLs at Site 977. The amended ORLs show a correlation with the Sea Surface Temperatures and the recognized climatic events over the Last Glacial Cycle in the Alboran Sea Basin.

The conducted integrative research improves the original definition of the ORLs based exclusively on colour contrast, magnetic susceptibility, and TOC, thus providing new insights to advance our understanding of ORL deposition in the Western Mediterranean.

Data availability

The available data for greyscale can be accessed in the supplementary material as "GreyScale 977".

Declaration of Competing Interest

The authors declare that they have no known competing financial interests or personal relationships that could have appeared to influence the work reported in this paper.

Acknowledgements

Research was funded by Projects CGL2015-66835-P, PID2019-104624RB-I00 and PID2019-104625RB-100 (Secretaría de Estado de I + D + I, Spain), and B-RNM-072-UGR18, P18-RT-3804 and P18-RT-4074 (Junta de Andalucía), and the Scientific Excellence Unit UCE-2016-05 (Universidad de Granada). The research of SC-A is funded through a pre-doctoral grant, FPU, from the Ministerio de Educación, Cultura y Deporte (Gobierno de España). The authors thank the Editor (Dr Rebesco) and both anonymous reviewers, whose comments helped improve the quality of this article. Funding for open access charge: Universidad de Granada/CBUA.

References

Aller, R.C., 1982. The effects of macrobenthos on chemical properties of marine sediment and overlying water. In: McCall, P.L., Tevesz, M.J.S. (Eds.), Animal-Sediment Relations. Topics in Geobiology, 100. Springer, Boston, MA, pp. 53–102. https://doi.org/10.1007/978-1-4757-1317-6_2.

Arndt, S., Jørgensen, B.B., LaRowe, D.E., Middelburg, J.J., Pancost, R.D., Regnier, P., 2013. Quantifying the degradation of organic matter in marine sediments: a review and synthesis. Earth Sci. Rev. 123, 53–86. https://doi.org/10.1016/j.earscirev.2013.02.008.

Ausín, B., Flores, J.A., Sierro, F.-J., Bárcena, M.Á., Hernández-Almeida, I., Francés, G., Gutiérrez-Arnillas, E., Martrat, B., Grimalt, J.O., Cacho, I., 2015a. Coccolithophore productivity and surface water dynamics in the Alboran Sea during the last 25kyr. Palaeogeogr. Palaeoclimatol. Palaeoecol. 418, 126–140. https://doi.org/10.1016/j.palaeo.2014.11.011.

Ausín, B., Flores, J.A., Sierro, F.J., Cacho, I., Hernández-Almeida, I., Martrat, B., Grimalt, J.O., 2015b. Atmospheric patterns driving Holocene productivity in the Alboran Sea (Western Mediterranean): a multiproxy approach. The Holocene 25, 583–595. https://doi.org/10.1177/0959683614565952.

Bahr, A., Kaboth, S., Jiménez-Espejo, F.J., Sierro, F.J., Voelker, A.H.L., Lourens, L., Röhl, U., Reichart, G.J., Escutia, C., Hernández-Molina, F.J., Pross, J., Friedrich, O., 2015. Persistent monsoonal forcing of Mediterranean Outflow Water dynamics during the late Pleistocene. Geology 43, 951–954. https://doi.org/10.1130/G37013.1.

Bárcena, M.Á., Cacho, I., Abrantes, F., Sierro, F.J., Grimalt, J., Flores, J., 2001. Paleoproductivity variations related to climatic conditions in the Alboran Sea (Western Mediterranean) during the last glacial-interglacial transition: the diatom record. Palaeogeogr. Palaeoclimatol. Palaeoecol. 167, 337–357. https://doi.org/10.1016/S0031-0182(00)00246-7.

Baringer, M.O.N., Price, J.F., 1999. A review of the physical oceanography of the Mediterranean outflow. Mar. Geol. 155 (1–2), 63–82. https://doi.org/10.1016/S0025-3227(98)00141-8.

Bar-Matthews, M., Ayalon, A., Kaufman, A., 2000. Timing and hydrological conditions of Sapropel events in the Eastern Mediterranean, as evident from speleothems, Soreq cave, Israel. Chem. Geol. 169 (1–2), 145–156. https://doi.org/10.1016/S0009-2541(99)00232-6.

Baucon, A., Bednarz, M., Dufour, S., Felletti, F., Malgesini, G., Neto de Carvalho, C., Niklas, K.J., Wehrmann, A., Batstone, R., Bernardini, F., Briguglio, A., Cabella, R., Cavalazzi, B., Ferretti, A., Zanzerl, H., Mcllroy, D., 2020. Ethology of the trace fossil *Chondrites*: form, function and environment. Earth Sci. Rev. 202, 102989. https://doi.org/10.1016/j.earscirev.2019.102989.

Bazzicalupo, P., Maiorano, P., Girone, A., Marino, M., Combourieu-Nebout, N., Incarbona, A., 2018. High-frequency climate fluctuations over the last deglaciation in the Alboran Sea, Western Mediterranean: evidence from calcareous plankton assemblages. Palaeogeogr. Palaeoclimatol. Palaeoecol. 506, 226–241. https://doi.org/10.1016/j.palaeo.2018.06.042.

Berner, R., 2003. The long-term carbon cycle, fossil fuels and atmospheric composition. Nature 426, 323–326. https://doi.org/10.1038/nature02131.

Bethoux, J.P., Gentili, B., 1999. Functioning of the Mediterranean Sea: past and present changes related to freshwater input and climate changes. J. Mar. Syst. 20, 33–47. https://doi.org/10.1016/S0924-7963(98)00069-4.

Bethoux, J.P., Gentili, B., Morin, P., Nicolas, E., Pierre, C., Ruiz-Pino, D., 1999. The Mediterranean Sea: a miniature ocean for climatic and environmental studies and a key for the climatic functioning of the North Atlantic. Prog. Oceanogr. 44, 131–146. https://doi.org/10.1016/S0079-6611(99)00023-3.

Blair, N.E., Aller, R.C., 2012. The Fate of Terrestrial Organic Carbon in the Marine Environment. Annu. Rev. Mar. Sci. 4, 401–423. https://doi.org/10.1146/annurev-marine-120709-142717.

Bromley, R.G., 2012. Trace Fossils: Biology, Taxonomy and Applications. Chapman & Hall, London, Glasgow, Weinheim, New York, Tokyo, Melbourne, Madras.

Bromley, R.G., Ekdale, A.A., Asgaard, U., 1999. Zoophycos in the Upper cretaceous chalk of Denmark and Sweden. Greifswalder Geowissenschaftliche Beiträge (ekkehard Herrig Festschrift) 6.

Buatois, L.A., Mángano, M.G., 2011. Ichnology. Cambridge University Press, Cambridge.

Cacho, I., Grimalt, J.O., Sierro, F.J., Shackleton, N., Canals, M., 2000. Evidence for enhanced Mediterranean thermohaline circulation during rapid climatic coolings. Earth Planet. Sci. Lett. 183, 417–429. https://doi.org/10.1016/S0012-821X(00)00296-X.

Cacho, I., Grimalt, J.O., Canals, M., 2002. Response of the Western Mediterranean Sea to rapid climatic variability during the last 50,000 years: a molecular biomarker approach. J. Mar. Syst. 33-34, 253–272. https://doi.org/10.1016/S0924-7963(02)00061-1.

Cacho, I., Shackleton, N., Elderfield, H., Sierro, F.J., Grimalt, J.O., 2006. Glacial rapid variability in deep-water temperature and δ18O from the Western Mediterranean Sea. Quat. Sci. Rev. 25, 3294–3311. https://doi.org/10.1016/j.quascirev.2006.10.004.

Calvert, S.E., 1987. Oceanographic controls on the accumulation of organic matter in marine sediments. Geol. Soc. London. Spec. Publ. 26, 137–151. https://doi.org/10.1144/GSL.SP.1987.026.01.08.

Canfield, D.E., 1994. Factors influencing organic carbon preservation in marine sediments. Chem. Geol. 114, 315–329. https://doi.org/10.1016/0009-2541(94)90061-2.

Carmona, N.B., Mángano, M.G., Buatois, L.A., Bromley, R.G., Ponce, J.J., Asgaard, U., Bellosi, E., 2020. *Scolicia* and its producer in shallow-marine deposits of the Miocene Chenque Formation (Patagonia, Argentina): functional morphology and implications for understanding burrowing behaviour. Ichnos 27, 290–299. https://doi.org/10.1080/10420940.2020.1744589.

Casanova-Arenillas, S., Rodríguez-Tovar, F.J., Martínez-Ruiz, F., 2020. Applied ichnology in sedimentary geology: Python scripts as a method to automatize ichnofabric analysis in marine core images. Comput. Geosci. 136, 104407. https://doi.org/10.1016/j.cageo.2020.104407.

Casanova-Arenillas, S., Rodríguez-Tovar, F.J., Martínez-Ruiz, F., 2021. Ichnological analysis as a tool for assessing deep-sea circulation in the westernmost Mediterranean over the last Glacial Cycle. Palaeogeogr. Palaeoclimatol. Palaeoecol. 562, 110082. https://doi.org/10.1016/j.palaeo.2020.110082.

Casford, J.S.L., Rohling, E., Abu-Zied, R., Fontanier, C., Jorissen, F., Leng, M., Schmiedl, G., Thomson, J., 2003. A dynamic concept for eastern Mediterranean circulation and oxygenation during sapropel formation. Palaeogeogr. Palaeoclimatol. Palaeoecol. 190, 103–119. https://doi.org/10.1016/S0031-0182(02)00601-6.

Cisneros, M., Cacho, I., Frigola, J., Sánchez-Vidal, A., Calafat, A., Pedrosa-Pàmies, R., Rumín-Caparrós, A., Canals, M., 2019. Deep-water formation variability in the North-Western Mediterranean Sea during the last 2500 yr: a proxy validation with present-day data. Glob. Planet. Chang. 177, 56–68. https://doi.org/10.1016/j.gloplacha.2019.03.012.

Combourieu Nebout, N., Peyron, O., Dormoy, I., Desprat, S., Beaudouin, C., Kotthoff, U., Marret, F., 2009. Rapid climatic variability in the West Mediterranean during the last 25 000 years from high resolution pollen data. Clim. Past 5 (3), 503–521. https://doi.org/10.5194/cp-5-503-2009.

Cramp, A., O'Sullivan, G., 1999. Neogene sapropels in the Mediterranean: a review. Mar. Geol. 153, 11–28. https://doi.org/10.1016/S0025-3227(98)00092-9.

Dansgaard, W., Johnsen, S.J., Clausen, H.B., Dahl-Jensen, D., Gundestrup, N.S., Hammer, C.U., Hvidberg, C.S., Steffensen, J.P., Sveinbjörnsdottir, A.E., Jouzel, J., Bond, G., 1993. Evidence for general instability of past climate from a 250-kyr ice-core record. Nature 364, 218–220. https://doi.org/10.1038/364218a0.

Dorador, J., Rodríguez-Tovar, F.J., 2014a. Quantitative estimation of bioturbation based on digital image analysis. Mar. Geol. 349, 55–60. https://doi.org/10.1016/j.margeo.2014.01.003.

Dorador, J., Rodríguez-Tovar, F.J., 2014b. Digital image treatment applied to ichnological analysis of marine core sediments. Facies 60, 39–44. https://doi.org/10.1007/s10347-013-0383-z.

Dorador, J., Rodríguez-Tovar, F.J., 2016. High resolution digital image treatment to color analysis on cores from IODP Expedition 339: Approaching lithologic features and bioturbational influence. Mar. Geol. 377, 127–135. https://doi.org/10.1016/j.margeo.2016.02.005.

Dorador, J., Rodríguez-Tovar, F.J., 2018. High-resolution image treatment in ichnological core analysis: initial steps, advances and prospects. Earth Sci. Rev. 177, 226–237. https://doi.org/10.1016/j.earscirev.2017.11.020.

Dorador, J., Wetzel, A., Rodríguez-Tovar, F.J., 2016. *Zoophycos* in deep-sea sediments indicates high and seasonal primary productivity: Ichnology as a proxy in palaeoceanography during glacial-interglacial variations. Terra Nova 28, 323–328. https://doi.org/10.1111/ter.12224.

Durrieu de Madron, X., Houpert, L., Puig, P., Sánchez-Vidal, A., Testor, P., Bosse, A., Estournel, C., Somot, S., Bourrin, F., Bouin, M., Beauverger, M., Beguery, L., Calafat, A., Canals, M., Cassou, C., Coppola, L., Dausse, D., D'Ortenzio, F., Font, J., Heussner, S., Kunesch, S., Lefevre, D., Le Goff, H., Martín, J., Mortier, L., Palanques, A., Raimbault, P., 2013. Interaction of dense shelf water cascading and open-sea convection in the northwestern Mediterranean during winter 2012. Geophys. Res. Lett. 40, 1379–1385. https://doi.org/10.1002/grl.50331.

Ehrenberg, K., 1944. Ergänzende Bemerkungen zu den seinerzeit aus dem Miozän von Burgschleinitz beschriebenen Gangkernen und Bauten dekapoder Krebse. Paläontol. Z. 23, 354–359. https://doi.org/10.1007/BF03160443.

Ekdale, A., Bromley, R.G., 2003. Paleoethologic interpretation of complex *Thalassinoides* in shallow-marine limestones, lower Ordovician, southern Sweden. Palaeogeogr. Palaeoclimatol. Palaeoecol. 192, 221–227. https://doi.org/10.1016/S0031-0182(02)00686-7.

Emeis, K.C., Sakamoto, T., Wehausen, R., Brumsack, H.-J., 2000. The sapropel record of the eastern Mediterranean Sea - results of Ocean Drilling Program Leg 160. Palaeogeogr. Palaeoclimatol. Palaeoecol. 158, 371–395. https://doi.org/10.1016/S0031-0182(00)00059-6.

Fischer, H., Fundel, F., Ruth, U., Twarloh, B., Wegner, A., Udisti, R., Becagli, S., Castellano, E., Morganti, A., Severi, M., Wolff, E., Littot, G., Röthlisberger, R., Mulvaney, R., Hutterli, M.A., Kaufmann, P., Federer, U., Lambert, F., Bigler, M., Hansson, M., Jonsell, U., de Angelis, M., Boutron, C., Siggaard-Andersen, M.L., Steffensen, J.P., Barbante, C., Gaspari, V., Gabrielli, P., Wagenbach, D., 2007. Reconstruction of millennial changes in dust emission, transport and regional sea ice coverage using the deep EPICA ice cores from the Atlantic and Indian Ocean sector of Antarctica. Earth Planet. Sci. Lett. 260, 340–354. https://doi.org/10.1016/j.epsl.2007.06.014.

Frey, R.W., Curran, A.H., Pemberton, S.G., 1984. Tracemaking activities of crabs and their environmental significance: the ichnogenus Psilonichnus. J. Paleontol. 511–528.

Frigola, J., Moreno, A., Cacho, I., Canals, M., Sierro, F.J., Flores, J.A., Grimalt, J.O., 2008. Evidence of abrupt changes in Western Mediterranean Deep Water circulation during the last 50kyr: a high-resolution marine record from the Balearic Sea. Quat. Int. 181, 88–104. https://doi.org/10.1016/j.quaint.2007.06.016.

von Grafenstein, R., Zahn, R., Tiedemann, R., Murat, A., 1999. Planktonic δ18O records at Sites 976 and 977, Alboran Sea: stratigraphy, forcing, and paleoceanographic implications. In: Zahn, R., Comas, M.C., Klays, A (Eds.), Proceedings of the Ocean Drilling Program Scientific, 161. Scientific Results, pp. 469–479.

Grant, K.M., Grimm, R., Mikolajewicz, U., Marino, G., Ziegler, M., Rohling, E.J., 2016. The timing of Mediterranean sapropel deposition relative to insolation, sea-level and African monsoon changes. Quat. Sci. Rev. 140, 125–141. https://doi.org/10.1016/j.quascirev.2016.03.026.

Grimm, R., Maier-Reimer, E., Mikolajewicz, U., Schmiedl, G., Müller-Navarra, K., Adloff, F., Emeis, K.C., 2015. Late glacial initiation of Holocene eastern Mediterranean sapropel formation. Nat. Commun. 6 (1), 1–12. https://doi.org/10.1038/ncomms8099.

Heburn, G.W., La Violette, P.E., 1990. Variations in the structure of the anticyclonic gyres found in the Alboran Sea. J. Geophys. Res. 95, 1599–1613. https://doi.org/10.1029/JC095iC02p01599.

Hedges, J.I., Keil, R.G., 1995. Sedimentary organic matter preservation: an assessment and speculative synthesis. Mar. Chem. 49, 81–115. https://doi.org/10.1016/0304-4203(95)00008-F.

Hedges, J.I., Keil, R.G., Benner, R., 1997. What happens to terrestrial organic matter in the ocean? Org. Geochem. 27, 195–212. https://doi.org/10.1016/S0146-6380(97)00066-1.

Hernández-Molina, F.J., Stow, D.A.V., Alvarez-Zarikian, C., Acton, G., Bahr, A., Balestra, B., Ducassou, E., Flood, R., Flores, J.-A., Furota, S., Grunert, P., Hodell, D. A., Jiménez-Espejo, F.J., Kim, J.K., Krissek, L., Kuroda, J., Li, B., Llave, E., Lofi, J., Lourens, L., Miller, M., Nanayama, F., Nishida, N., Richter, C., Roque, C., Pereira, H., Sánchez Goñi, M.F., Sierro, F.J., Singh, A.D., Sloss, C., Takashimizu, Y., Tzanova, A., Voelker, A., Williams, T., Xuan, C., 2014. Onset of Mediterranean outflow into the North Atlantic. Science (80) 344, 1244–1250. https://doi.org/10.1126/science.1251306.

Hertweck, G., Wehrmann, A., Liebezeit, G., 2007. Bioturbation structures of polychaetes in modern shallow marine environments and their analogues to *Chondrites* group traces. Palaeogeogr. Palaeoclimatol. Palaeoecol. 245, 382–389. https://doi.org/10.1016/j.palaeo.2006.09.001.

Hodell, D.A., Nicholl, J.A., Bontognali, T.R.R., Danino, S., Dorador, J., Dowdeswell, J.A., Einsle, J., Kuhlmann, H., Martrat, B., Mleneck-Vautravers, M.J., Rodríguez-Tovar, F. J., Röhl, U., 2017. Anatomy of Heinrich Layer 1 and its role in the last deglaciation. Paleoceanography 32, 284–303. https://doi.org/10.1002/2016PA003028.

Hunter, J., Dale, D., Firing, E., Droettboo, M., 2012. Matplotlib: Python Plotting [WWW Document]. Matplotlib.Org.

Incarbona, A., Sprovieri, M., 2020. The postglacial isotopic record of intermediate water connects Mediterranean Sapropels and Organic-Rich Layers. Paleoceanogr. Paleoclimatol. 35 (10) https://doi.org/10.1029/2020PA004009 e2020PA004009.

Jenkyns, H.C., 2010. Geochemistry of oceanic anoxic events. Geochem. Geophys. Geosyst. 11 https://doi.org/10.1029/2009GC002788.

Jiménez-Espejo, F.J., Pardos-Gené, M., Martínez-Ruiz, F., García-Alix, A., van de Flierdt, T., Toyofuku, T., Bahr, A., Kreissig, K., 2015. Geochemical evidence for intermediate water circulation in the westernmost Mediterranean over the last 20kyrBP and its impact on the Mediterranean Outflow. Glob. Planet. Chang. 135, 38–46. https://doi.org/10.1016/j.gloplacha.2015.10.001.

Jung, M., Ilmberger, J., Mangini, A., Emeis, K.-C., 1997. Why some Mediterranean sapropels survived burn-down (and others did not). Mar. Geol. 141, 51–60. https://doi.org/10.1016/S0025-3227(97)00031-5.

Keighley, D.G., Pickerill, R.K., 1995. The ichnotaxa *Palaeophycus* and *Planolites*: Historical perspectives and recommendations. Ichnos 3, 301–309.

Kidd, R.B., Cita, M.B., Ryan, W.B.F., 1978. Stratigraphy of eastern Mediterranean sapropel sequences recovered during Leg 42A and their paleoenvironmental significance. Initial Reports Deep-Sea Drill. Proj. 42A, 421–443.

Knaust, D., 2017. Atlas of Trace Fossils in Well Core. Springer International Publishing, Cham.

Kotake, N., 2014. Changes in lifestyle and habitat of*Zoophycos*-producing animals related to evolution of phytoplankton during the Late Mesozoic: geological evidence for the 'benthic-pelagic coupling model'. Lethaia 47, 165–175. https://doi.org/10.1111/let.12046.

Kuypers, M.M.M., Pancost, R.D., Nijenhuis, I.A., Sinninghe Damsté, J.S., 2002. Enhanced productivity led to increased organic carbon burial in the euxinic North Atlantic basin during the late Cenomanian oceanic anoxic event. Paleoceanography 17, 1–13. https://doi.org/10.1029/2000PA000569.

LaRowe, D.E., Arndt, S., Bradley, J.A., Estes, E.R., Hoarfrost, A., Lang, S.Q., Lloyd, K.G., Mahmoudi, N., Orsi, W.D., Shah Walter, S.R., Steen, A.D., Zhao, R., 2020. The fate of organic carbon in marine sediments - New insights from recent data and analysis. Earth Sci. Rev. 204, 103146. https://doi.org/10.1016/j.earscirev.2020.103146.

Larrasoaña, J.C., Roberts, A.P., Hayes, A., Wehausen, R., Rohling, E.J., 2006. Detecting missing beats in the Mediterranean climate rhythm from magnetic identification of oxidized sapropels (Ocean Drilling Program Leg 160). Phys. Earth Planet. Inter. 156, 283–293. https://doi.org/10.1016/j.pepi.2005.04.017.

Łaska, W., Rodríguez-Tovar, F.J., Uchman, A., 2017. Evaluating macrobenthic response to the Cretaceous-Palaeogene event: a high-resolution ichnological approach at the Agost section (SE Spain). Cretac. Res. 70, 96–110. https://doi.org/10.1016/j.cretres.2016.10.003.

Lionello, P. (Ed.), 2012. The Climate of the Mediterranean Region: From the Past to the Future, 1st ed. Elsevier Insights, Elsevier Science, Amsterdam.

Löwemark, L., 2012. Ethological analysis of the trace fossil *Zoophycos*: hints from the Arctic Ocean. Lethaia 45, 290–298. https://doi.org/10.1111/j.1502-3931.2011.00282.x.

Löwemark, L., 2015. Testing ethological hypotheses of the trace fossil *Zoophycos* based on Quaternary material from the Greenland and Norwegian Seas. Palaeogeogr. Palaeoclimatol. Palaeoecol. 425, 1–13. https://doi.org/10.1016/j.palaeo.2015.02.025.

Löwemark, L., Lin, Y., Chen, H.F., Yang, T.N., Beier, C., Werner, F., Lee, C.Y., Song, S.R., Kao, S.J., 2006. Sapropel burn-down and ichnological response to late Quaternary sapropel formation in two ~ 400 ky records from the eastern Mediterranean Sea. Palaeogeogr. Palaeoclimatol. Palaeoecol. 239, 406–425. https://doi.org/10.1016/j.palaeo.2006.02.013.

Magwood, J.P.A., Ekdale, A.A., 1994. Computer-aided analysis of visually complex Ichnofabrics in deep-sea sediments. Palaios 9, 102–115. https://doi.org/10.2307/3515083.

Martínez-Ruiz, F., Kastner, M., Gallego-Torres, D., Rodrigo-Gámiz, M., Nieto-Moreno, V., Ortega-Huertas, M., 2015. Paleoclimate and paleoceanography over the past 20,000 yr in the Mediterranean Sea Basins as indicated by sediment elemental proxies. Quat. Sci. Rev. 107, 25–46. https://doi.org/10.1016/j.quascirev.2014.09.018.

Martrat, B., Grimalt, J.O., López-Martínez, C., Cacho, I., Sierro, F.J., Flores, J.A., Zahn, R., Canals, M., Curtis, J.H., Hodell, D.A., 2004. Abrupt Temperature changes in the Western Mediterranean over the past 250,000 years. Science (80) 306, 1762–1765. https://doi.org/10.1126/science.1101706.

Martrat, B., Grimalt, J.O., Shackleton, N.J., De Abreu, L., Hutterli, M.A., Stocker, T.F., 2007. Four climate cycles of recurring deep and surface water destabilizations on the Iberian margin. Science (80) 317, 502–507. https://doi.org/10.1126/science.1139994.

Martrat, B., Jimenez-Amat, P., Zahn, R., Grimalt, J.O., 2014. Similarities and dissimilarities between the last two deglaciations and interglaciations in the North Atlantic region. Quat. Sci. Rev. 99, 122–134. https://doi.org/10.1016/j.quascirev.2014.06.016.

Massalongo, A., 1855. *Zoophycos*, novum genus plantarum fossilium. Monographia. Typis Antonellianis, Veronae, pp. 45–52.

Mavropoulou, A.M., Vervatis, V., Sofianos, S., 2020. Dissolved oxygen variability in the Mediterranean Sea. J. Mar. Syst. 208, 103348. https://doi.org/10.1016/j.jmarsys.2020.103348.

Medoc Group, Lacombe, H., Tehernia, P., Ribet, M., Bonnot, J., Frassetto, R., Swallow, J. C., Miller, A.R., Stommel, H., 1970. Observation of Formation of Deep Water in the Mediterranean Sea, 1969. Nature 227, 1037–1040. https://doi.org/10.1038/2271037a0.

Meyers, P.A., Arnaboldi, M., 2005. Trans-Mediterranean comparison of geochemical paleoproductivity proxies in a mid-Pleistocene interrupted sapropel. Palaeogeogr. Palaeoclimatol. Palaeoecol. 222, 313–328. https://doi.org/10.1016/j.palaeo.2005.03.020.

Middelburg, J.J., 1989. A simple rate model for organic matter decomposition in marine sediments. Geochim. Cosmochim. Acta 53, 1577–1581. https://doi.org/10.1016/0016-7037(89)90239-1.

Middelburg, J.J., 2018. Reviews and syntheses: to the bottom of carbon processing at the seafloor. Biogeosciences 15, 413–427. https://doi.org/10.5194/bg-15-413-2018.

Middelburg, J.J., Nieuwenhuize, J., Van Breugel, P., 1999. Black carbon in marine sediments. Mar. Chem. 65, 245–252. https://doi.org/10.1016/S0304-4203(99)00005-5.

Miguez-Salas, O., Rodríguez-Tovar, F.J., Duarte, L.V., 2017. Selective incidence of the Toarcian oceanic anoxic event on macroinvertebrate marine communities: a case from the Lusitanian basin, Portugal. Lethaia 50, 548–560. https://doi.org/10.1111/let.12212.

Miguez-Salas, O., Rodríguez-Tovar, F.J., Duarte, L.V., 2018. Ichnological analysis at the Fonte Coberta section (Lusitanian Basin, Portugal): Approaching depositional environment during the Toarcian oceanic anoxic event (T-OAE). Spanish J. Palaeontol. 33, 261–276.

Millot, C., 1999. Circulation in the Western Mediterranean Sea. J. Mar. Syst. 20, 423–442. https://doi.org/10.1016/S0924-7963(98)00078-5.

Millot, C., 2014. Heterogeneities of in-and out-flows in the Mediterranean Sea. Prog. Oceanogr. 120, 254–278. https://doi.org/10.1016/j.pocean.2013.09.007.

Millot, C., Taupier-Letage, I., 2005. Circulation in the Mediterranean Sea. In: Saliot, A. (Ed.), The Mediterranean Sea. Handbook of Environmental Chemistry. Springer, Berlin, Heidelberg, pp. 29–66.

Mollenhauer, G., Inthorn, M., Vogt, T., Zabel, M., Sinninghe Damsté, J.S., Eglinton, T.I., 2007. Aging of marine organic matter during cross-shelf lateral transport in the Benguela upwelling system revealed by compound-specific radiocarbon dating. Geochem. Geophys. Geosyst. 8 https://doi.org/10.1029/2007GC001603.

Monaco, P., Rodríguez-Tovar, F.J., Uchman, A., 2012. Ichnological analysis of lateral environmental heterogeneity within the Bonarelli Level (Uppermost Cenomanian) in the classical localities near Gubbio, central apennines, Italy. Palaios 27, 48–54. https://doi.org/10.2110/palo.2011.p11-018r.

Monaco, P., Rodríguez-Tovar, F.J., Uchman, A., 2016. Environmental fluctuations during the latest Cenomanian (Bonarelli Level) in the Gubbio area (Central Italy) based on an ichnofabric approach. In: The Geological Society of America Special Papper, 524, pp. 97–103.

Moodley, L., Middelburg, J.J., Herman, P.M.J., Soetaert, K., de Lange, G.J., 2005. Oxygenation and organic-matter preservation in marine sediments: Direct experimental evidence from ancient organic carbon-rich deposits. Geology 33, 889–892. https://doi.org/10.1130/G21731.1.

Müller, P.J., Suess, E., 1979. Productivity, sedimentation rate, and sedimentary organic matter in the oceans—I. Organic carbon preservation. Deep Sea Res. Part A. Oceanogr. Res. Pap. 26, 1347–1362. https://doi.org/10.1016/0198-0149(79)90003-7.

Murat, A., 1999. Pliocene-Pleistocene occurrence of sapropels in the Western Mediterranean Sea and their relation to eastern Mediterranean sapropels. In: Zahn, R., Comas, M.C., Klaus, A. (Eds.), Proceedings of the Ocean Drilling Program, Scientific Results., 161 Ocean Drilling Program, pp. 519–527.

Naranjo, C., García Lafuente, J., Sánchez Garrido, J.C., Sánchez Román, A., Delgado Cabello, J., 2012. The western alboran gyre helps ventilate the western mediterranean deep water through Gibraltar. Deep. Res. Part I Oceanogr. Res. Pap. 63, 157–163. https://doi.org/10.1016/j.dsr.2011.10.003.

Naranjo, C., Sammartino, S., García-Lafuente, J., Bellanco, M.J., Taupier-Letage, I., 2015. Mediterranean waters along and across the Strait of Gibraltar, characterization and zonal modification. Deep. Res. Part I Oceanogr. Res. Pap. 105, 41–52. https://doi.org/10.1016/j.dsr.2015.08.003.

Nicholson, H.A., 1873. Contributions to the study of the Errant Anelides of the older Paleozoic rocs. Proc. R. Soc. Lond. 21, 299–290.

Nickell, L., Atkinson, R., 1995. Functional morphology of burrows and trophic modes of three thalassinidean shrimp species, and a new approach to the classification of thalassinidean burrow morphology. Mar. Ecol. Prog. Ser. 128, 181–197.

Pedersen, T.F., Calvert, S.E., 1990. Anoxia vs. productivity: what controls the formation of organic-carbon-rich sediments and sedimentary rocks? Am. Assoc. Pet. Geol. Bull. 74, 454–466. https://doi.org/10.1306/0C9B232B-1710-11D7-8645000102C1865D.

Pemberton, S.G., Frey, R.W., 1982. Trace fossil nomenclature and the*Planolites-Palaeophycus* dilemma. J. Paleontol. 56, 843–881. http://www.jstor.org/stable/1304706.

Pérez-Asensio, J.N., Frigola, J., Pena, L.D., Sierro, F.J., Reguera, M.I., Rodríguez-Tovar, F.J., Dorador, J., Asioli, A., Kuhlmann, J., Huhn, K., Cacho, I., 2020. Changes in western Mediterranean thermohaline circulation in association with a deglacial Organic Rich Layer formation in the Alboran Sea. Quat. Sci. Rev. 228, 106075. https://doi.org/10.1016/j.quascirev.2019.106075.

Pérez-Folgado, M., Sierro, F.J., Flores, J.A., Grimalt, J.O., Zahn, R., 2004. Paleoclimatic variations in foraminifer assemblages from the Alboran Sea (Western Mediterranean) during the last 150 ka in ODP Site 977. Mar. Geol. 212, 113–131. https://doi.org/10.1016/j.margeo.2004.08.002.

Pinardi, N., Masetti, E., 2000. Variability of the large scale general circulation of the Mediterranean Sea from observations and modelling: a review. Palaeogeogr. Palaeoclimatol. Palaeoecol. 158, 153–173. https://doi.org/10.1016/S0031-0182(00)00048-1.

Pinardi, N., Zavatarelli, M., Adani, M., Coppini, G., Fratianni, C., Oddo, P., Simoncelli, S., Tonani, M., Lyubartsev, V., Dobricic, S., Bonaduce, A., 2015. Mediterranean Sea large-scale low-frequency ocean variability and water mass formation rates from 1987 to 2007: a retrospective analysis. Prog. Oceanogr. 132, 318–332. https://doi.org/10.1016/j.pocean.2013.11.003.

Quatrefages, M.A., 1849. Note sur la *Scolicia prisca* (A. de Q.) annélide fossile de la Craie. Ann. des Sci. Nat. 3 série. Zool. 12, 265–266.

Rasmussen, S.O., Bigler, M., Blockley, S.P., Blunier, T., Buchardt, S.L., Clausen, H.B., Cvijanovic, I., Dahl-Jensen, D., Johnsen, S.J., Fischer, H., Gkinis, V., Guillevic, M., Hoek, W.Z., Lowe, J.J., Pedro, J.B., Popp, T., Seierstad, I.K., Steffensen, J.P., Svensson, A.M., Vallelonga, P., Vinther, B.M., Walker, M.J.C., Wheatley, J.J., Winstrup, M., 2014. A stratigraphic framework for abrupt climatic changes during the last Glacial period based on three synchronized Greenland ice-core records: refining and extending the INTIMATE event stratigraphy. Quat. Sci. Rev. 106, 14–28. https://doi.org/10.1016/j.quascirev.2014.09.007.

Reolid, M., Emanuela, M., Nieto, L.M., Rodríguez-Tovar, F.J., 2014. The early Toarcian Oceanic Anoxic Event in the External Subbetic (Southiberian Palaeomargin, Westernmost Tethys): geochemistry, nannofossils and ichnology. Palaeogeogr. Palaeoclimatol. Palaeoecol. 411, 79–94. https://doi.org/10.1016/j.palaeo.2014.06.023.

Rhein, M., 1995. Deep water formation in the western Mediterranean. J. Geophys. Res. 100, 6943. https://doi.org/10.1029/94JC03198.

Rodrigo-Gámiz, M., Martínez-Ruiz, F., Jiménez-Espejo, F.J., Gallego-Torres, D., Nieto-Moreno, V., Romero, O., Ariztegui, D., 2011. Impact of climate variability in the western Mediterranean during the last 20,000 years: oceanic and atmospheric responses. Quat. Sci. Rev. 30, 2018–2034. https://doi.org/10.1016/j.quascirev.2011.05.011.

Rodrigo-Gámiz, M., Martínez-Ruiz, F., Rodríguez-Tovar, F.J., Jiménez-Espejo, F.J., Pardo-Igúzquiza, E., 2014. Millennial- to centennial-scale climate periodicities and forcing mechanisms in the westernmost Mediterranean for the past 20,000 yr. Quat. Res. 81, 78–93. https://doi.org/10.1016/j.yqres.2013.10.009.

Rodríguez-Tovar, F.J., 2021. Ichnology of the Toarcian Oceanic Anoxic Event: an understimated tool to assess palaeoenvironmental interpretations. Earth Sci. Rev. 216, 103579. https://doi.org/10.1016/j.earscirev.2021.103579.

Rodríguez-Tovar, F.J., Dorador, J., 2014. Ichnological analysis of Pleistocene sediments from the IODP Site U1385 "Shackleton Site" on the Iberian margin: approaching paleoenvironmental conditions. Palaeogeogr. Palaeoclimatol. Palaeoecol. 409, 24–32. https://doi.org/10.1016/j.palaeo.2014.04.027.

Rodríguez-Tovar, F.J., Dorador, J., 2015. Ichnofabric characterization in cores: a method of digital image treatment. Ann. Soc. Geol. Pol. 85, 465–471. https://doi.org/10.14241/asgp.2015.010.

Rodríguez-Tovar, F.J., Uchman, A., 2010. Ichnofabric evidence for the lack of bottom anoxia during the lower Toarcian oceanic anoxic event in the Fuente de la Vidriera section, Betic Cordillera, Spain. Palaios 25, 576–587. https://doi.org/10.2110/palo.2009.p09-153r.

Rodríguez-Tovar, F.J., Uchman, A., 2011. Ichnological data as a useful tool for deep-sea environmental characterization: a brief overview and an application to recognition of small-scale oxygenation changes during the Cenomanian-Turonian anoxic event. Geo-Marine Lett. 31, 525–536. https://doi.org/10.1007/s00367-011-0237-z.

Rodríguez-Tovar, F.J., Uchman, A., 2017. The Faraoni event (latest Hauterivian) in ichnological record: the Río Argos section of southern Spain. Cretac. Res. 79, 109–121. https://doi.org/10.1016/j.cretres.2017.07.018.

Rodríguez-Tovar, F.J., Uchman, A., Martín-Algarra, A., 2009. Oceanic Anoxic Event at the Cenomanian-Turonian boundary interval (OAE-2): ichnological approach from the Betic Cordillera, southern Spain. Lethaia 42, 407–417. https://doi.org/10.1111/j.1502-3931.2009.00159.x.

Rodríguez-Tovar, F.J., Dorador, J., Grunert, P., Hodell, D.A., 2015. Deep-sea trace fossil and benthic foraminiferal assemblages across glacial Terminations 1, 2 and 4 at the "Shackleton Site" (IODP Expedition 339, Site U1385). Glob. Planet. Chang. 133, 359–370. https://doi.org/10.1016/j.gloplacha.2015.05.003.

Rodríguez-Tovar, F.J., Miguez-Salas, O., Duarte, L.V., 2017. Toarcian Oceanic Anoxic Event induced unusual behaviour and palaeobiological changes in *Thalassinoides* tracemakers. Palaeogeogr. Palaeoclimatol. Palaeoecol. 485, 46–56. https://doi.org/10.1016/j.palaeo.2017.06.002.

Rodríguez-Tovar, F.J., Dorador, J., Mena, A., Hernández-Molina, F.J., 2018. Lateral variability of ichnofabrics in marine cores: improving sedimentary basin analysis using Computed Tomography images and high-resolution digital treatment. Mar. Geol. 397, 72–78. https://doi.org/10.1016/j.margeo.2017.12.006.

Rodríguez-Tovar, F.J., Hernández-Molina, F.J., Hüneke, H., Llave, E., Stow, D., 2019a. Contourite facies model: improving contourite characterization based on the ichnological analysis. Sediment. Geol. 384, 60–69. https://doi.org/10.1016/j.sedgeo.2019.03.010.

Rodríguez-Tovar, F.J., Miguez-Salas, O., Dorador, J., Duarte, L.V., 2019b. Opportunistic behaviour after the Toarcian Oceanic Anoxic Event: the trace fossil *Halimedides*. Palaeogeogr. Palaeoclimatol. Palaeoecol. 520, 240–250.

Rodríguez-Tovar, F.J., Dorador, J., Mena, A., Francés, G., 2020a. Regional and global changes during Heinrich Event 1 affecting macrobenthic habitat: Ichnological evidence of sea-bottom conditions at the Galicia Interior Basin. Glob. Planet. Chang. 192 https://doi.org/10.1016/j.gloplacha.2020.103227.

Rodríguez-Tovar, F.J., Uchman, A., Reolid, M., Sánchez-Quiñónez, C.A., 2020b. Ichnological analysis of the Cenomanian-Turonian boundary interval in a collapsing slope setting: a case from the Rio Fardes section, southern Spain. Cretac. Res. 106, 104262. https://doi.org/10.1016/j.cretres.2019.104262.

Rogerson, M., Cacho, I., Jímenez-Espejo, F., Reguera, M.I., Sierro, F.J., Martínez-Ruiz, F., Frigola, J., Canals, M., 2008. A dynamic explanation for the origin of the western Mediterranean organic-rich layers. Geochem. Geophys. Geosyst. 9, Q07U01.

Rohling, E.J., 1994. Review and new aspects concerning the formation of eastern Mediterranean sapropels. Mar. Geol. 122, 1–28. https://doi.org/10.1016/0025-3227(94)90202-X.

Rohling, E.J., Hilgen, F.J., 1991. The eastern Mediterranean climate at times of sapropel formation. Geol. Mijnb. 70, 252–264.

Rohling, E.J., Marino, G., Grant, K.M., 2015. Mediterranean climate and oceanography, and the periodic development of anoxic events (sapropels). Earth Sci. Rev. 143, 62–97. https://doi.org/10.1016/j.earscirev.2015.01.008.

Rossignol-Strick, M., Paterne, M., 1999. A synthetic pollen record of the eastern Mediterranean sapropels of the last 1 Ma: implications for the time-scale and formation of sapropels. Mar. Geol. 153 (1–4), 221–237. https://doi.org/10.1016/S0025-3227(98)00080-2.

Sánchez Goñi, M.F., Ferretti, P., Polanco-Martínez, J.M., Rodrigues, T., Alonso-García, M., Rodríguez-Tovar, F.J., Dorador, J., Desprat, S., 2019. Pronounced northward shift of the westerlies during MIS 17 leading to the strong 100-kyr ice age cycles. Earth Planet. Sci. Lett. 511, 117–129. https://doi.org/10.1016/j.epsl.2019.01.032.

Sarhan, T., 2000. Upwelling mechanisms in the northwestern Alboran Sea. J. Mar. Syst. 23, 317–331. https://doi.org/10.1016/S0924-7963(99)00068-8.

Savrda, C.E., 2007. Trace fossils and marine benthic oxygenation. In: Trace Fossils. Elsevier, pp. 149–158. https://doi.org/10.1016/B978-044452949-7/50135-2.

Savrda, C.E., Bottjer, D.J., 1986. Trace-fossil model for reconstruction of paleo-oxygenation in bottom waters. Geology 14, 3–6. https://doi.org/10.1130/0091-7613(1986)14<3:TMFROP>2.0.CO;2.

Savrda, C.E., Bottjer, D.J., 1987. Trace fossils as indicators of bottom-water redox conditions in ancient marine environments. In: New Concepts in the use of Biogenic Sedimentary Structures for Paleoenvironmental Interpretation: volume and Guidebook. Pacific Section SEPM, pp. 3–26.

Savrda, C.E., Bottjer, D.J., 1989. Trace-fossil model for reconstructing oxygenation histories of ancient marine bottom waters: application to Upper Cretaceous Niobrara formation. Colorado. Palaeogeogr. Palaeoclimatol. Palaeoecol. 74, 49–74. https://doi.org/10.1016/0031-0182(89)90019-9.

Savrda, C.E., Bottjer, D.J., 2008. Oxygen-related biofacies in marine strata: an overview and update. Geol. Soc. London Spec. Publ. 58, 201–219. https://doi.org/10.1144/GSL.SP.1991.058.01.14.

Schindelin, J., Arganda-Carreras, I., Frise, E., Kaynig, V., Longair, M., Pietzsch, T., Preibisch, S., Rueden, C., Saalfeld, S., Schmid, B., Tinevez, J.-Y., White, D.J., Hartenstein, V., Eliceiri, K., Tomancak, P., Cardona, A., 2012. Fiji: an open-source platform for biological-image analysis. Nat. Methods 9, 676–682. https://doi.org/10.1038/nmeth.2019.

Schlirf, M., 2000. Upper Jurassic trace fossils from the Boulonnais (northern France). Geol. Palaeontol. 34, 145–213.

Schroeder, K., Ribotti, A., Borghini, M., Sorgente, R., Perilli, A., Gasparini, G.P., 2008. An extensive western Mediterranean deep water renewal between 2004 and 2006. Geophys. Res. Lett. 35, L18605 https://doi.org/10.1029/2008GL035146.

Schroeder, K., Garcìa-Lafuente, J., Josey, S.A., Artale, V., Nardelli, B.B., Carrillo, A., Gačić, M., Gasparini, G. Pietro, Herrmann, M., Lionello, P., Ludwig, W., Millot, C., Özsoy, E., Pisacane, G., Sánchez-Garrido, J.C., Sannino, G., Santoleri, R., Somot, S., Struglia, M., Stanev, E., Taupier-Letage, I., Tsimplis, M.N., Vargas-Yáñez, M., Zervakis, V., Zodiatis, G., 2012. Circulation of the Mediterranean Sea and its Variability. In: The Climate of the Mediterranean Region. Elsevier, pp. 187–256.

Shipboard Scientific Party, 1996a. Site 976. In: Proceedings of the Ocean Drilling Program, 161 Initial Reports. Ocean Drilling Program.

Shipboard Scientific Party, 1996b. Site 977. In: Proceedings of the Ocean Drilling Program, 161 Initial Reports. Ocean Drilling Program.

Sierro, F.J., Hodell, D.A., Curtis, J.H., Flores, J.A., Reguera, I., Colmenero-Hidalgo, E., Bárcena, M.Á., Grimalt, J.O., Cacho, I., Frigola, J., Canals, M., 2005. Impact of iceberg melting on Mediterranean thermohaline circulation during Heinrich events. Paleoceanography 20, PA2019. https://doi.org/10.1029/2004PA001051.

Sigl, W., Chamley, H., Fabricius, F., Ghislaine, G. d'Argoud, Müller, J., 1978. Sedimentology and environmental conditions of sapropels. In: Initial Reports 42 Part 1, 42. Deep Sea Drilling Project, pp. 445–465.

Somot, S., Houpert, L., Sevault, F., Testor, P., Bosse, A., Taupier-Letage, I., Bouin, M., Waldman, R., Cassou, C., Sánchez-Gomez, E., Durrieu de Madron, X., Adloff, F., Nabat, P., Herrmann, M., 2018. Characterizing, modelling and understanding the climate variability of the deep water formation in the North-Western Mediterranean Sea. Clim. Dyn. 51, 1179–1210. https://doi.org/10.1007/s00382-016-3295-0.

von Sternberg, K.G., 1833. Versuch einer geognostisch- botanischen Darstellung der Flora der Vorwelt, 1. Fr. Fleischer, Leipzig, Prague, pp. 5–8.

Tyson, R.V., 2001. Sedimentation rate, dilution, preservation and total organic carbon: some results of a modelling study. Org. Geochem. 32 (2), 333–339. https://doi.org/10.1016/S0146-6380(00)00161-3.

Tyson, R.V., Pearson, T.H., 1991. Modern and ancient continental shelf anoxia: an overview. Geol. Soc. Spec. Publ. 58, 1–24. https://doi.org/10.1144/GSL.SP.1991.058.01.01.

Uchman, A., Wetzel, A, 2011. Deep-sea ichnology: the relationships between depositional environment and endobenthic organisms. In: Developments in Sedimentology. Elsevier, pp. 517–556. https://doi.org/10.1016/B978-0-444-53000-4.00008-1.

Uchman, A., Wetzel, A., 2012. Deep-sea fans. In: Developments in Sedimentology. Elsevier, pp. 643–671. https://doi.org/10.1016/B978-0-444-53813-0.00021-6.

Uchman, A., Bak, K., Rodríguez-Tovar, F.J., 2008. Ichnological record of deep-sea palaeoenvironmental changes around the Oceanic Anoxic Event 2 (Cenomanian-Turonian boundary): an example from the Barnasiówka section, Polish Outer Carpathians. Palaeogeogr. Palaeoclimatol. Palaeoecol. 262, 61–71. https://doi.org/10.1016/j.palaeo.2008.02.002.

Uchman, A., Rodríguez-Tovar, F.J., Machaniec, E., Kędzierski, M., 2013a. Ichnological characteristics of late cretaceous hemipelagic and pelagic sediments in a submarine high around the OAE-2 event: a case from the Rybie section, Polish Carpathians. Palaeogeogr. Palaeoclimatol. Palaeoecol. 370, 222–231. https://doi.org/10.1016/j.palaeo.2012.12.013.

Uchman, A., Rodríguez-Tovar, F.J., Oszczypko, N., 2013b. Exceptionally favourable life conditions for macrobenthos during the late Cenomanian OAE-2 event: Ichnological record from the Bonarelli Level in the Grajcarek Unit, Polish Carpathians. Cretac. Res. 46, 1–10. https://doi.org/10.1016/j.cretres.2013.08.007.

Wetzel, A., 1991. Ecologic interpretation of deep-sea trace fossil communities. Palaeogeogr. Palaeoclimatol. Palaeoecol. 85, 47–69. https://doi.org/10.1016/0031-0182(91)90025-M.

Wetzel, A., 2008. Recent bioturbation in the deep South China Sea: a uniformitarian ichnologic approach. Palaios 23, 601–615. https://doi.org/10.2110/palo.2007.p07-096r.

Wetzel, A., 2010. Deep-sea ichnology: Observations in modern sediments to interpret fossil counterparts. Acta Geol. Pol. 60, 125–138.

Wetzel, A., Uchman, A., 2012. Hemipelagic and Pelagic Basin Plains. In: Developments in Sedimentology, 65. Elsevier, pp. 673–701. https://doi.org/10.1016/B978-0-444-53813-0.00022-8.

Wu, Jiawang, Filippidi, Amalia, Davies, Gareth R., de Lange, Gert J., 2018. Riverine supply to the eastern Mediterranean during last interglacial sapropel S5 formation: A basin-wide perspective. Chem. Geol. 485, 74–89. https://doi.org/10.1016/j.chemgeo.2018.03.037.

Wüst, G., 1961. On the vertical circulation of the Mediterranean Sea. J. Geophys. Res. 66, 3261–3271. https://doi.org/10.1029/JZ066i010p03261.

Zonneveld, K.A.F., Versteegh, G.J.M., Kasten, S., Eglinton, T.I., Emeis, K.-C., Huguet, C., Koch, B.P., de Lange, G.J., de Leeuw, J.W., Middelburg, J.J., Mollenhauer, G., Prahl, F.G., Rethemeyer, J., Wakeham, S.G., 2010. Selective preservation of organic matter in marine environments; processes and impact on the sedimentary record. Biogeosciences 7, 483–511. https://doi.org/10.5194/bg-7-483-2010.